PNNL-26057, Rev 0.0
EWG-RPT-011, Rev 0.0

Pacific Northwest
NATIONAL LABORATORY
Proudly Operated by Battelle Since 1965

Results from Phase 1, 2, and 3 Studies on Nepheline Formation in High-Level Waste Glasses Containing High Concentrations of Alumina

November 2016

J.O. Kroll
J.D. Vienna
M.J. Schweiger
G.F. Piepel
S.K. Cooley

U.S. DEPARTMENT OF ENERGY
Prepared for the U.S. Department of Energy under Contract DE-AC05-76RL01830

PACIFIC NORTHWEST NATIONAL LABORATORY
operated by
BATTELLE
for the
UNITED STATES DEPARTMENT OF ENERGY
under Contract DE-AC05-76RL01830

Printed in the United States of America

Available to DOE and DOE contractors from the
Office of Scientific and Technical Information,
P.O. Box 62, Oak Ridge, TN 37831-0062;
ph: (865) 576-8401
fax: (865) 576-5728
email: reports@adonis.osti.gov

Available to the public from the National Technical Information Service
5301 Shawnee Rd., Alexandria, VA 22312
ph: (800) 553-NTIS (6847)
email: orders@ntis.gov <http://www.ntis.gov/about/form.aspx>
Online ordering: http://www.ntis.gov

This document was printed on recycled paper.
(8/2010)

PNNL-26057, Rev 0.0
EWG-RPT-011, Rev. 0.0

Results from Phase 1, 2, and 3 Studies on Nepheline Formation in High-Level Waste Glasses Containing High Concentrations of Alumina

J.O. Kroll
J.D. Vienna
M.J. Schweiger
G.F. Piepel
S.K. Cooley

November 2016

Prepared for
the U.S. Department of Energy
under Contract DE-AC05-76RL01830

Pacific Northwest National Laboratory
Richland, Washington 99352

Acknowledgments

Pacific Northwest National Laboratory (PNNL) is operated by Battelle under Contract Number DE-AC05-76RL01830. The authors are grateful for the financial support provided by the U.S. Department of Energy Office of River Protection's (ORP) Hanford Tank Waste Treatment and Immobilization Plant Federal Project Office under the direction of William F. Hamel, Jr. The programmatic guidance of Albert Kruger (ORP) is greatly appreciated. The scientific discussions and guidance of Dong-Sang Kim, Pavel Hrma, and Jesse Lang (all from PNNL) are appreciated. The authors would also like to thank Kevin Fox of Savannah River National Laboratory for the analytical laboratory support and Product Consistency Test measurements. Additionally, the authors would like to thank Cary Counts (from PNNL) for support with the technical editing and formatting of this report.

Summary

The composition of Hanford high-level waste (HLW) is dominated by relatively high concentrations of Al_2O_3. A major constraint limiting the waste loading of high-Al_2O_3 glasses is nepheline (nominally $NaAlSiO_4$) formation upon slow cooling of HLW glasses after melts are poured into canisters. The model currently planned to be used at the Hanford Tank Waste Treatment and Immobilization Plant (WTP) for avoiding nepheline formation is too conservative and drastically limits waste loading.[1] To increase loadings of high-Al_2O_3 waste at the WTP, the effects of glass composition on glass properties must be determined and glass property-composition models must be developed.[2] An important task of this effort is determining the impacts of glass composition on nepheline formation and the effects of nepheline on Product Consistency Test (PCT) response.

As a part of this task, data related to the Hanford high-Al_2O_3 HLW composition region were generated. Forty-five glasses were fabricated, heat treated, analyzed for crystallinity, and tested for PCT response. The heat treatment was designed to mimic the canister centerline cooling (CCC) profile of Hanford HLW canisters.[3] X-ray diffraction was used to quantify the crystal fractions of the CCC samples. The PCT was performed at the Savannah River National Laboratory and normalized releases of B, Si, Na, and Li (g/L) reported.[4] In addition, composition analyses of the glasses were performed to support comparing the targeted and analyzed compositions of each glass.[4]

A review of the data showed a strong correlation between the fraction of nepheline formed during CCC and PCT responses. Generally, as the fraction of nepheline increased, so did the PCT releases of B, Na, and Li.

[1] Vienna, JD, D-S Kim, DC Skorski, and J Matyas. 2013. *Glass Property Models and Constraints for Estimating the Glass to Be Produced at Hanford by Implementing Current Advanced Glass Formulation Efforts.* PNNL-22631, (ORP-58289) Rev. 1, Pacific Northwest National Laboratory, Richland, Washington. Available at http://www.pnnl.gov/main/publications/external/technical_reports/PNNL-22631Rev1.pdf.

[2] Peeler, DK, JD Vienna, MJ Schweiger, and KM Fox. 2015. *Advanced High-Level Waste Glass Research and Development Plan.* PNNL-24450, Pacific Northwest National Laboratory Richland, Washington. Available at http://www.pnnl.gov/main/publications/external/technical_reports/PNNL-24450.pdf.

[3] Petkus, L. October 19, 2003. "Canister Centerline Cooling Data, 24590-PADC-F00029 Rev 1." *Memorandum to C. Musick.* River Protection Project, Waste Treatment Plant,. Richland, Washington.

[4] Fox, KM, TB Edwards, and D L McClane. 2016. *Chemical Composition Analysis and Product Consistency Tests Supporting Refinement of the Nepheline Model for the High Aluminum Hanford Glass Composition Region*. SRNL-STI-2016-00028, Rev. 1, Savannah River National Laboratory, Aiken, South Carolina.

Acronyms and Abbreviations

2CAT	two-components-at-a-time
3CAT	three-components-at-a-time
AD	acid dissolution
ARM-1	Approved Reference Material number one
BDL	below detectable limit
CC	collection code
CCC	canister centerline cooling
DOE	U.S. Department of Energy
DWPF	Defense Waste Processing Facility
EA	environmental assessment
EU	eucryptite
EWG	enhanced waste glass
FIO	for information only
HLW	high-level waste
ICP-OES	inductively coupled plasma – optical emission spectroscopy
ICSD	Inorganic Crystal Structure Database
LAW	low-activity waste
LRM	low-activity reference material
ND	nepheline discriminator
NN	neural network
NP	nepheline
NQAP	PNNL Nuclear Quality Assurance Program
OB	optical basicity
OCAT	one-component-at-a-time
ORP	U.S. Department of Energy, Office of River Protection
PCT	Product Consistency Test
PF	peroxide fusion
PNNL	Pacific Northwest National Laboratory
QA	quality assurance
SRNL	Savannah River National Laboratory
WTP	Hanford Tank Waste Treatment and Immobilization Plant
XRD	x-ray diffraction

Contents

Acknowledgments iii
Summary v
Acronyms and Abbreviations vii
1.0 Introduction 1.1
2.0 Quality Assurance 2.1
2.1 PNNL Quality Assurance Program 2.1
2.2 EWG QA Program 2.1
3.0 Experimental Design 3.1
3.1 Phase 1 Design 3.1
3.2 Phase 2 Design 3.5
3.3 Phase 3 Design 3.5
3.3.1 Generating 2CAT and 3CAT Glass Compositions 3.5
3.3.2 Selecting an Optimal Subset of 2CAT and 3CAT Compositions for the Phase 3 Study 3.7
4.0 Experimental Methods 4.1
4.1 Glass Fabrication 4.1
4.2 Canister Centerline Cooling Heat Treatment 4.1
4.3 X-ray Diffraction Analysis 4.2
4.4 Composition Analysis 4.2
4.5 Product Consistency Test 4.3
5.0 Results 5.1
5.1 X-ray Diffraction Crystal Fraction Results 5.1
5.2 Composition Analysis Results 5.6
5.3 Product Consistency Test Results 5.7
6.0 Discussion and Conclusions 6.1
7.0 References 7.1
Appendix A Quantitative XRD Results for Major Crystalline Phases A.1
Appendix B XRD Spectrum for the Glass with Unfit Peaks B.1
Appendix C Composition Analysis Results C.1

Figures

3.1 Scatterplot Matrix of Al_2O_3, B_2O_3, Li_2O, Na_2O, and SiO_2 Component Mass Fractions for the Phase 3 Glasses and the Phase 1 and Phase 2 Glasses Inside the Phase 3 Glass Composition Region 3.10

6.1 Measured Mass Fractions of Nepheline and Eucryptite in Glasses vs. Component Differences from the BL3 Baseline Glass 6.2

6.2 Measured mass% of Crystal vs Normalized PCT Release of (a) B, (b) Li, and (c) Na 6.3

6.3 Natural Logarithm of Normalized B Release of Quenched Glasses Subtracted from the Natural Logarithm of Normalized B Release of CCC Glasses Plotted Against Measured mass% of Nepheline and/or Eucryptite 6.4

B.1 XRD Pattern from NP-MC-AlBSi-1 CCC Sample B.1

Tables

3.1 Targeted Component Lower and Upper Bounds (mass fractions) for Glass Composition Regions Investigated in Phases 1, 2, and 3 ..... 3.2

3.2 Targeted Compositions (mass fractions) for Phases 1, 2, and 3 ..... 3.3

3.3 Targeted Compositions (mass fractions) for the 21 Existing Glasses within the Phase 3 Composition Region 3.9

4.1 CCC Heat Treatment Schedule 4.1

5.1 XRD Crystal Percentage Results in Mass% 5.1

5.2 PCT Results for Quenched and CCC Glasses Normalized to the Targeted Compositions 5.9

A.1 Quantitative XRD Results for all Major Crystalline Phases A.2

C.1 Composition Analysis Results Including Reference Material C.1

1.0 Introduction

The U.S. Department of Energy (DOE) will immobilize in borosilicate glass the roughly 200,000 m^3 of radioactive waste stored in underground tanks on the Hanford site. The Hanford Tank Waste Treatment and Immobilization Plant (WTP) is currently being constructed to accomplish this task. The WTP will segregate high-level waste (HLW) and low-activity waste (LAW) fractions, blend each with glass forming chemicals, melt the mixtures at ~1150°C, and pour the molten glasses into stainless steel canisters to cool and solidify (DOE 2000).

According to the 2008 HLW feed vector reported by Vienna et al. (2013), many HLW compositions contain high concentrations of Al_2O_3. The Al_2O_3 fraction is projected to range from roughly 10 to 70 mass% on a calcined oxide basis after caustic leaching.

The loading of high-Al_2O_3 HLW's may be drastically reduced by the constraint(s) applied to reduce the probability of forming nepheline (nominally $NaAlSiO_4$) upon slow cooling of glasses. Nepheline precipitation from a HLW glass during cooling is a major concern because it will likely reduce the durability of the resulting glass by removing three moles of glass former oxides (one mole of Al_2O_3 and two moles of SiO_2) for every mole of Na_2O (Kim et al. 1995). When nepheline is present in a waste glass, it is difficult to predict the Product Consistency Test (PCT) (ASTM 2014) response (Peeler et al. 2015). It has also been documented that eucryptite ($LiAlSiO_4$) has a similar effect on glass durability (McCloy and Vienna 2010). To meet disposal requirements, nepheline formation must be avoided, or the amount of nepheline formed and its impact on the PCT response must be predicted. Being able to predict the amount of nepheline formed and the PCT response would provide a basis for specifying a constraint to avoid HLW glass compositions that would yield unacceptable PCT response.

The current model used to avoid nepheline formation is too conservative and limits waste loading (Vienna et al. 2016). A nepheline discriminator (ND) was developed to reduce the risk of nepheline precipitation during canister centerline cooling (CCC) heat treatment (Li et al. 1997). This approach is based on limiting the normalized SiO_2 concentration (N_{Si}) using the inequality

$$N_{Si} = \frac{g_{SiO_2}}{g_{SiO_2} + g_{Al_2O_3} + g_{Na_2O}} < 0.62 \tag{1.1}$$

Here, g_i is the mass fraction of the i^{th} component in the glass. The ND predicts that glasses with $N_{Si} < 0.62$ are prone to nepheline crystallization during CCC heat treatment.

In an effort to reduce some of the conservatism in the ND, optical basicity (OB) was proposed as a constraint (Rodriguez et al. 2011, McCloy et al. 2011). The revised constraint allows glasses with $N_{Si} < 0.62$ as long as the OB of the melt is less than 0.55. The OB of a glass (Λ_{glass}) can be calculated from a glass composition using

$$\Lambda_{glass} = \frac{\sum_i x_i q_i \Lambda_i}{\sum_i x_i q_i} \tag{1.2}$$

where

q_i = the number of oxygen atoms in the i^{th} component oxide

x_i = the mole fraction of the i^{th} component oxide in glass

Λ_i = the molar basicity of the i^{th} component oxide

This approach did reduce some of the conservatism, but still limits the waste loading of high-Al_2O_3 glasses (Vienna et al. 2016).

A neural network (NN) model has also been proposed to estimate the probability of nepheline formation for a specific glass composition (Vienna et al. 2013). This approach was selected because it can account for highly non-linear effects of components. The NN model consists of three nodes using the hyperbolic tangent (TanH) transfer function. The output from the three nodes was compared to a probability cutoff value to assign a binary response (i.e., whether nepheline formed or not) for a glass composition. However, the NN method involves complex calculations and determining the uncertainties of predictions made with the model would be difficult (Vienna et al. 2016).

To optimize waste loading, a new approach is needed to limit nepheline precipitation during slow cooling of HLW canisters. It has been demonstrated that B_2O_3, CaO, Fe_2O_3, K_2O, and Li_2O affect nepheline formation (Li et al. 1997). A ternary sub-mixture model that takes advantage of the success of the ND while considering the effects of other components in the melt has been developed (Vienna et al. 2016). New data are needed to refine and validate this model or to develop improved models. This report describes several new test matrices of HLW glasses and nepheline formation results that will be used to supplement existing data in models to predict the formation of nepheline, the amount of nepheline formed, and/or the PCT responses of glasses forming nepheline.

2.0 Quality Assurance

2.1 PNNL Quality Assurance Program

The PNNL Quality Assurance (QA) Program was adhered to during the conduct of the Phase 1, Phase 2, and Phase 3 studies of this work. This program is based on the requirements as defined in the DOE Order 414.1D, *Quality Assurance*, and 10 CFR 830, *Energy/Nuclear Safety Management*, Subpart A, *Quality Assurance Requirements* (a.k.a., the Quality Rule). PNNL has chosen to implement the following consensus standards in a graded approach:

- ASME NQA-1-2000, *Quality Assurance Requirements for Nuclear Facility Applications*, Part I, "Requirements for Quality Assurance Programs for Nuclear Facilities"
- ASME NQA-1-2000, Part II, Subpart 2.7, "Quality Assurance Requirements for Computer Software for Nuclear Facility Applications," including problem reporting and corrective action
- ASME NQA-1-2000, Part IV, Subpart 4.2, "Guidance on Graded Application of Quality Assurance (QA) for Nuclear-Related Research and Development."

The PNNL *Quality Assurance Program Description/Quality Management M&O Program Description* describes the laboratory-level QA program that applies to all work performed by PNNL. Laboratory-level procedures for implementing the QA requirements described in the standards identified above are deployed through PNNL's web-based "How Do I…?" system, which is a standards-based system for managing and deploying requirements and procedures to PNNL staff. The procedures (called Workflows and Work Controls) provide detailed guidance for performing some types of tasks, such as protecting classified information and procuring items and services, as well as general guidelines for performing research-related tasks, such as preparing and reviewing calculations and calibrating and controlling measuring and test equipment.

2.2 Enhanced Waste Glass Quality Assurance Program

Until May 31, 2016, the Enhanced Waste Glass Project (EWG) used the Washington River Protection Solutions Waste Form Testing Program (WWFTP) QA program as the basis for performing work. The WWFTP QA program implements the requirements of NQA-1-2008, Quality Assurance Requirements for Nuclear Facility Applications, and NQA-1a-2009, Addenda to ASME NQA-1-2008, Quality Assurance Requirements for Nuclear Facility Applications, graded on the approach presented in NQA-1-2008, Part IV, Subpart 4.2.

On June 1, 2016, EWG transferred to the PNNL Nuclear Quality Assurance Program (NQAP). This QA program is compliant with ASME-NQA-1-2012, 10 CFR 830, Subpart A, DOE Order (O) 414.1D, and is for use by research and development (R&D) projects and programs that are compatible with the editions of ASME NQA-1 2000 through 2012. The work described in this report was performed to the QA level of Applied Research, which is defined below:

> *"…nuclear and non-nuclear R&D (work activities or deliverables) that are processes initiated-with-the-intent of solving a specific problem or meeting a practical need. For applied research activities, grading is minimal and largely contingent upon the complexity of the research and the ability to*

duplicate the research if data were lost. The elements of QA grading, including the level of documentation, were applied to the program-, project-, and task-levels."

The HLW nepheline study Phase 1, Phase 2, and Phase 3 test matrices were generated under the WWFTP QA program. The generation of the Phase 1 and Phase 2 matrices is documented in Calculation Packages EWG-CCP-023 and EWG-CCP-024, respectively. Calculation Package EWG-CCP-024 also documents the computation of NP2-High Na*, which was adjusted from the targeted glass composition (NP2-High Na) due to a likely misbatch (discussed in Section 5.2). The possible misbatch of NP2-High Na is documented in the corrective action report EWG-CAR-O3670. The PCT results associated with NP2-High Na were renormalized to the adjusted composition (NP2-High Na*); this is documented in EWG-CCP-025. The generation of the Phase 3 test matrix using statistical methods is documented in Calculation Packages CCP-EWG-018 and CCP-EWG-019.

Analytical results associated with test instructions TI-EWG-0018 (Phase 2 study) and TI-EWG-0019 (Phase 3 study) were qualified as acceptable through the "Qualifying Existing Data" process documented in EWG-DQP-0004 and EWG-DQR-0009 for TI-EWG-0018 and EWG-DQP-0005 and EWG-DQR-0005 for TI-EWG-0019.

All of the laboratory work and testing associated with the Phase 1 study did not adhere to the WWFTP QA program except in the case of glass Neph-NN-1-12. The results associated with Neph-NN-1-12 were qualified as acceptable through the "Qualifying Existing Data" process documented in EWG-DQP-0001 and EWG-DQR-0001. All other results from the Phase 1 study are considered for information only (FIO).

The calculations performed to construct Figure 6.3 were not reviewed as required by the WWFTP-QA, and the information provided in the figure is considered FIO.

3.0 Experimental Design

This section discusses three new phases of experimental design work for high-Al_2O_3 HLW glasses to (i) investigate the effects of key HLW glass components affecting nepheline formation, (ii) generate data to develop and validate models for nepheline formation and nepheline fraction, and (iii) investigate the effects of nepheline fraction on PCT response.

3.1 Phase 1 Experimental Design

The Phase 1 experimental design was developed around a baseline glass (BL0) roughly in the center of the predicted Hanford high-Al_2O_3 HLW glass composition region. The HLW glasses in this composition region met all property constraints for fabrication in the WTP (described in Vienna et al. 2013) without any constraint for nepheline formation.

A set of 15 glasses were then developed by adjusting Al_2O_3, B_2O_3, CaO, Fe_2O_3, Li_2O, Na_2O, and SiO_2 one-component-at-a-time (OCAT) from their values in the BL0 composition. Each OCAT change in a component was offset by changes to the remaining glass components, keeping them in the same relative proportions as in the BL0 baseline glass, so that the component mass fractions summed to unity. These OCAT changes and the offsetting changes in the remaining components were calculated using

$$g_i = g_{Bi} + \Delta_i \qquad g_h = g_{Bh} - \frac{\Delta_i g_{Bh}}{1 - g_{Bi}} \quad h \neq i \tag{3.1}$$

where

- g_i = mass fraction of the i^{th} glass component after the Δ_i OCAT change
- g_{Bi} = mass fraction of the i^{th} glass component in the baseline composition
- Δ_i = OCAT change in the i^{th} glass component ($g_i - g_{Bi}$), which can be positive or negative
- g_h = mass fraction of the h^{th} glass component after the change to offset the Δ_i OCAT change in the i^{th} component
- g_{Bh} = mass fraction of the h^{th} glass component in the baseline composition.

Table 3.1 lists the targeted component lower and upper bounds (mass fractions) investigated during Phase 1. The 15 glasses in the Phase 1 experimental design were then selected such that the OCAT changes did not exceed these lower and upper bounds. The glass identifiers (IDs) and targeted compositions of the 15 Phase 1 glasses are listed in Table 3.2. All of the values listed in Tables 3.1 and 3.2 are targeted values, not measured.

Table 3.1. Targeted Component Lower and Upper Bounds (mass fractions) for HLW Glass Composition Regions Investigated in Nepheline Study Phases 1, 2, and 3. Values shown in boldface are for the components directly varied within a given study.

		Phase 1			Phase 2		Phase 3				
Component	**BL0**	**Lower Bound**	**Upper Bound**	**BL3**	**Lower Bound**	**Upper Bound**	**Lower Bound**	**Upper Bound**	**BL1**	**BL2**	**BL4**
Al_2O_3	0.2850	**0.266**[(a)]	**0.3043**[(a)]	0.2850	**0.2541**[(b)]	**0.3450**	**0.2550**	**0.3150**	0.2900	0.2850	0.2850
B_2O_3	0.1800	**0.1400**	**0.2200**	0.1720	**0.1400**	**0.2200**	**0.1400**	**0.2200**	0.1640	0.1700	0.1700
Bi_2O_3	0.0075	0.007	0.0080	0.0065	0.0058	0.0072	0.0053	0.0078	0.0070	0.0065	0.0065
CaO	0.0050	0.0047[(c)]	**0.0700**	0.0065	0.0058	0.0072	0.0053	0.0078	0.0070	0.0065	0.0065
Cr_2O_3	0.0050	0.0047	0.0053	0.0110	0.0098	0.0121	0.0090	0.0132	0.0100	0.0110	0.0110
F	0.0000	0.0000	0.0000	0.0030	0.0030	0.0033	0.0025	0.0036	0.0035	0.0030	0.0030
Fe_2O_3	0.0250	0.0234[(d)]	**0.0800**	0.0250	0.0223	0.0276	0.0205	0.0299	0.0250	0.0250	0.0250
Li_2O	0.0600	**0.0000**	**0.0641**[(e)]	0.0500	**0.0400**	**0.0600**	**0.0400**	**0.0600**	0.0400	0.0400	0.0400
MnO	0.0100	0.0093	0.0107	0.0100	0.0089	0.0110	0.0082	0.0120	0.0100	0.0100	0.0100
Na_2O	0.1000	**0.0800**	**0.1500**	0.1250	**0.0950**	**0.1550**	**0.0950**	**0.1550**	0.1500	0.1405	0.1305
NiO	0.0025	0.0023	0.0027	0.0000	0.0000	0.0000	0.0000	0.0000	0.0000	0.0000	0.0000
P_2O_5	0.0100	0.0093	0.0107	0.0070	0.0062	0.0077	0.0058	0.0084	0.0075	0.0070	0.0070
RuO_2	0.0005	0.0005	0.0005	0.0005	0.0004	0.0006	0.0004	0.0006	0.0005	0.0005	0.0005
SiO_2	0.3070	**0.2600**	**0.3266**[(f)]	0.2935	**0.2200**	**0.3700**	**0.2600**	**0.3300**	0.2800	0.2900	0.3000
SO_3	0.0025	0.0023	0.0027	0.0025	0.0022	0.0028	0.0021	0.0030	0.0025	0.0025	0.0025
ZrO_2	0.0000	0.0000	0.0000	0.0025	0.0022	0.0028	0.0021	0.0030	0.0030	0.0025	0.0025

(a) In Phase 1, Al_2O_3 was varied OCAT from 0.27 to 0.30 (see Table 3.2). Variations of other components OCAT yielded Al_2O_3 values lower than 0.27 and larger than 0.30.

(b) In Phase 2, Al_2O_3 was varied OCAT from 0.255 to 0.345 (see Table 3.2). Variations of other components OCAT yielded Al_2O_3 values lower than 0.255.

(c) In Phase 1, CaO was varied OCAT from 0.035 to 0.07 (see Table 3.2). Values of CaO in all other glass compositions varied below and above the BL0 baseline value for CaO of 0.005.

(d) In Phase 1, Fe_2O_3 was varied OCAT from 0.05 to 0.08 (see Table 3.2). Values of Fe_2O_3 in all other glass compositions varied below and above the BL0 baseline value for Fe_2O_3 of 0.025.

(e) In Phase 1, Li_2O was varied OCAT from its baseline value of 0.06 to values of 0 and 0.03. Values of Li_2O in all other glass compositions varied below and above the BL0 baseline value for Li_2O of 0.06.

(f) In Phase 1, SiO2 was varied to high value of 0.32. Variations of other components OCAT yielded SiO_2 values larger than 0.32.

Table 3.2. Targeted HLW Glass Compositions (mass fractions) for Nepheline Study Phases 1, 2, and 3. Values shown in boldface are for the components directly varied within a given study.

Glass ID	Phase	Al_2O_3	B_2O_3	Bi_2O_3	CaO	Cr_2O_3	F	Fe_2O_3	Li_2O	MnO	Na_2O	NiO	P_2O_5	RuO_2	SiO_2	SO_3	ZrO_2	Sum[a]	MT[b] (°C)
Neph-NN-1-01[c]	1	0.2850	0.1800	0.0075	0.0050	0.0050	0.0000	0.0250	0.0600	0.0100	0.1000	0.0025	0.0100	0.0005	0.3070	0.0025	0.0000	1.0000	1250
Neph-NN-1-02	1	**0.3000**	0.1762	0.0073	0.0049	0.0049	0.0000	0.0245	0.0587	0.0098	0.0979	0.0024	0.0098	0.0005	0.3006	0.0024	0.0000	0.9999	1200
Neph-NN-1-03	1	**0.2700**	0.1838	0.0077	0.0051	0.0051	0.0000	0.0255	0.0613	0.0102	0.1021	0.0026	0.0102	0.0005	0.3134	0.0026	0.0000	1.0001	1225
Neph-NN-1-04	1	0.2711	**0.2200**	0.0071	0.0048	0.0048	0.0000	0.0238	0.0571	0.0095	0.0951	0.0024	0.0095	0.0005	0.2920	0.0024	0.0000	1.0001	1140
Neph-NN-1-05	1	0.2989	**0.1400**	0.0079	0.0052	0.0052	0.0000	0.0262	0.0629	0.0105	0.1049	0.0026	0.0105	0.0005	0.3220	0.0026	0.0000	0.9999	1300
Neph-NN-1-06	1	0.2664	0.1682	0.0070	**0.0700**	0.0047	0.0000	0.0234	0.0561	0.0093	0.0935	0.0023	0.0093	0.0005	0.2869	0.0023	0.0000	0.9999	1140
Neph-NN-1-07	1	0.2764	0.1746	0.0073	**0.0350**	0.0048	0.0000	0.0242	0.0582	0.0097	0.0970	0.0024	0.0097	0.0005	0.2977	0.0024	0.0000	0.9999	1200
Neph-NN-1-08	1	0.2689	0.1698	0.0071	0.0047	0.0047	0.0000	**0.0800**	0.0566	0.0094	0.0944	0.0024	0.0094	0.0005	0.2897	0.0024	0.0000	1.0000	1390
Neph-NN-1-09	1	0.2777	0.1754	0.0073	0.0049	0.0049	0.0000	**0.0500**	0.0585	0.0097	0.0974	0.0024	0.0097	0.0005	0.2991	0.0024	0.0000	0.9999	1240
Neph-NN-1-10	1	0.2941	0.1857	0.0077	0.0052	0.0052	0.0000	0.0258	**0.0300**	0.0103	0.1032	0.0026	0.0103	0.0005	0.3168	0.0026	0.0000	1.0000	1390
Neph-NN-1-11	1	0.3032	0.1915	0.0080	0.0053	0.0053	0.0000	0.0266	**0.0000**	0.0106	0.1064	0.0027	0.0106	0.0005	0.3266	0.0027	0.0000	1.0000	1500
Neph-NN-1-12	1	0.2692	0.1700	0.0071	0.0047	0.0047	0.0000	0.0236	0.0567	0.0094	**0.1500**	0.0024	0.0094	0.0005	0.2899	0.0024	0.0000	1.0000	1150
Neph-NN-1-13	1	0.2913	0.1840	0.0077	0.0051	0.0051	0.0000	0.0256	0.0613	0.0102	**0.0800**	0.0026	0.0102	0.0005	0.3138	0.0026	0.0000	1.0000	1280
Neph-NN-1-14	1	0.2797	0.1766	0.0074	0.0049	0.0049	0.0000	0.0245	0.0589	0.0098	0.0981	0.0025	0.0098	0.0005	**0.3200**	0.0025	0.0000	1.0001	1270
Neph-NN-1-15	1	0.3043	0.1922	0.0080	0.0053	0.0053	0.0000	0.0267	0.0641	0.0107	0.1068	0.0027	0.0107	0.0005	**0.2600**	0.0027	0.0000	1.0000	1190
BL3	2	0.2850	0.1720	0.0065	0.0065	0.0110	0.0030	0.0250	0.0500	0.0100	0.1250	0.0000	0.0070	0.0005	0.2935	0.0025	0.0025	1.0000	1150
NP2-High Al	2	**0.3150**	0.1648	0.0062	0.0062	0.0105	0.0029	0.0240	0.0479	0.0096	0.1198	0.0000	0.0067	0.0005	0.2812	0.0024	0.0024	1.0001	1200
NP2-High B	2	0.2685	**0.2200**	0.0061	0.0061	0.0104	0.0028	0.0236	0.0471	0.0094	0.1178	0.0000	0.0066	0.0005	0.2765	0.0024	0.0024	1.0002	1150
NP2-High Li	2	0.2820	0.1702	0.0064	0.0064	0.0109	0.0030	0.0247	**0.0600**	0.0099	0.1237	0.0000	0.0069	0.0005	0.2904	0.0025	0.0025	1.0000	1150
NP2-High Na[d]	2	0.2752	0.1661	0.0063	0.0063	0.0106	0.0029	0.0241	0.0483	0.0097	**0.1550**	0.0000	0.0068	0.0005	0.2834	0.0024	0.0024	1.0000	1150
NP2-High Na*[d]	2	0.2746	0.1657	0.0063	0.0063	0.0106	0.0029	0.0241	0.0482	0.0096	**0.1546**	0.0000	0.0067	0.0005	0.2828	0.0024	0.0048	1.0001	1150
NP2-High Si	2	0.2703	0.1631	0.0062	0.0062	0.0104	0.0028	0.0237	0.0474	0.0095	0.1185	0.0000	0.0066	0.0005	**0.3300**	0.0024	0.0024	1.0000	1200
NP2-Low Al	2	**0.2550**	0.1792	0.0068	0.0068	0.0115	0.0031	0.0260	0.0521	0.0104	0.1302	0.0000	0.0073	0.0005	0.3058	0.0026	0.0026	0.9999	1150
NP2-Low B	2	0.2960	**0.1400**	0.0068	0.0068	0.0114	0.0031	0.0260	0.0519	0.0104	0.1298	0.0000	0.0073	0.0005	0.3048	0.0026	0.0026	1.0000	1200
NP2-Low Li	2	0.2880	0.1738	0.0066	0.0066	0.0111	0.0030	0.0253	**0.0400**	0.0101	0.1263	0.0000	0.0071	0.0005	0.2966	0.0025	0.0025	1.0000	1200
NP2-Low Na	2	0.2948	0.1779	0.0067	0.0067	0.0114	0.0031	0.0259	0.0517	0.0103	**0.0950**	0.0000	0.0072	0.0005	0.3036	0.0026	0.0026	1.0000	1200
NP2-Low Si	2	0.2985	0.1802	0.0068	0.0068	0.0115	0.0031	0.0262	0.0524	0.0105	0.1309	0.0000	0.0073	0.0005	**0.2600**	0.0026	0.0026	0.9999	1150
NP2-Very High Al	2	**0.3450**	0.1576	0.0060	0.0060	0.0101	0.0027	0.0229	0.0458	0.0092	0.1145	0.0000	0.0064	0.0005	0.2689	0.0023	0.0023	1.0002	1200
NP2-Very High Si	2	0.2541	0.1534	0.0058	0.0058	0.0098	0.0027	0.0223	0.0446	0.0089	0.1115	0.0000	0.0062	0.0004	**0.3700**	0.0022	0.0022	0.9999	1200
NP2-Very Low Si	2	0.3146	0.1899	0.0072	0.0072	0.0121	0.0033	0.0276	0.0552	0.0110	0.1380	0.0000	0.0077	0.0006	**0.2200**	0.0028	0.0028	1.0000	1150

Table 3.2. Targeted HLW Glass Compositions (mass fractions) for Nepheline Study Phases 1, 2, and 3. Values shown in boldface are for the components directly varied within a given study. (cont'd)

Glass ID	Phase	Al_2O_3	B_2O_3	Bi_2O_3	CaO	Cr_2O_3	F	Fe_2O_3	Li_2O	MnO	Na_2O	NiO	P_2O_5	RuO_2	SiO_2	SO_3	ZrO_2	Sum[a]	MT[b] (°C)
NP-MC-AlB-1	3	**0.2550**	**0.2200**	0.0063	0.0063	0.0106	0.0029	0.0242	0.0483	0.0097	0.1209	0.0000	0.0068	0.0005	0.2838	0.0024	0.0024	1.0001	1150
NP-MC-AlBNa-1	3	**0.2680**	**0.1539**	0.0073	0.0073	0.0124	0.0034	0.0281	0.0562	0.0112	**0.1080**	0.0000	0.0079	0.0006	0.3300	0.0028	0.0028	0.9999	1250
NP-MC-AlBNa-2	3	**0.2983**	**0.1932**	0.0058	0.0058	0.0097	0.0027	0.0221	0.0443	0.0089	**0.1383**	0.0000	0.0062	0.0004	0.2600	0.0022	0.0022	1.0001	1200
NP-MC-AlBSi-1	3	**0.3150**	**0.2200**	0.0053	0.0053	0.0090	0.0025	0.0205	0.0411	0.0082	0.1027	0.0000	0.0058	0.0004	**0.2600**	0.0021	0.0021	1.0000	1250
NP-MC-AlLi-1	3	**0.2550**	0.1823	0.0069	0.0069	0.0117	0.0032	**0.0265**	0.0400	0.0106	0.1325	0.0000	0.0074	0.0005	0.3112	0.0027	0.0027	1.0001	1200
NP-MC-AlLi-2	3	**0.3150**	0.1668	0.0063	0.0063	0.0107	0.0029	**0.0242**	0.0400	0.0097	0.1212	0.0000	0.0068	0.0005	0.2847	0.0024	0.0024	0.9999	1300
NP-MC-AlLiNa-1	3	**0.3114**	0.1524	0.0058	0.0058	0.0097	0.0027	0.0221	**0.0588**	0.0089	**0.1514**	0.0000	0.0062	0.0004	0.2600	0.0022	0.0022	1.0000	1150
NP-MC-AlLiSi-1	3	**0.2550**	0.2060	0.0078	0.0078	0.0132	0.0036	0.0299	**0.0400**	0.0120	0.1497	0.0000	0.0084	0.0006	**0.2600**	0.0030	0.0030	1.0000	1150
NP-MC-AlNa-1	3	**0.2550**	0.1720	0.0065	0.0065	0.0110	0.0030	0.0250	0.0500	0.0100	**0.1550**	0.0000	0.0070	0.0005	0.2935	0.0025	0.0025	1.0000	1150
NP-MC-AlSi-1	3	**0.2550**	0.1979	0.0075	0.0075	0.0127	0.0035	0.0288	0.0575	0.0115	0.1438	0.0000	0.0081	0.0006	**0.2600**	0.0029	0.0029	1.0002	1150
NP-MC-AlSi-2	3	**0.3150**	0.1449	0.0055	0.0055	0.0093	0.0025	0.0211	0.0421	0.0084	0.1053	0.0000	0.0059	0.0004	**0.3300**	0.0021	0.0021	1.0001	1350
NP-MC-BLiSi-1	3	0.2765	**0.1400**	0.0063	0.0063	0.0107	0.0029	0.0243	**0.0600**	0.0097	0.1213	0.0000	0.0068	0.0005	**0.3300**	0.0024	0.0024	1.0001	1200
NP-MC-BLiSi-2	3	0.2706	**0.2200**	0.0062	0.0062	0.0104	0.0028	0.0237	**0.0600**	0.0095	0.1187	0.0000	0.0066	0.0005	**0.2600**	0.0024	0.0024	1.0000	1150
NP-MC-BNa-1	3	0.2858	**0.1400**	0.0065	0.0065	0.0110	0.0030	0.0251	0.0501	0.0100	**0.1550**	0.0000	0.0070	0.0005	0.2943	0.0025	0.0025	0.9998	1200
NP-MC-BNaSi-1	3	0.3097	**0.1400**	0.0071	0.0071	0.0120	0.0033	0.0272	0.0543	0.0109	**0.1550**	0.0000	0.0076	0.0005	**0.2600**	0.0027	0.0027	1.0001	1150
NP-MC-BSi-1[e]	3	0.2550	**0.2040**	0.0058	0.0058	0.0098	0.0027	0.0224	0.0447	0.0089	0.1118	0.0000	0.0063	0.0005[e]	**0.3178**	0.0022	0.0022	0.9999	1200

(a) The component mass fraction values were calculated to more decimal places and summed to unity. However, rounding to four decimal places for this table led to sums different from 1.0000 by ±0.0002.

(b) MT = melt temperature.

(c) Neph-NN-1-01 is BL0

(d) Glass NP2-High Na is the target composition originally selected for the Phase 2 experimental design. However, it was subsequently determined that the glass was misbatched, so the final adjusted composition is listed as NP2-High Na*. It is this final adjusted composition that is recommended for modeling purposes.

(e) The RuO_2 mass fraction in glass NP-MC-BSi-1 was incorrectly rounded to 0.0005 rather than 0.0004, but makes no practical difference.

3.2 Phase 2 Experimental Design

Phase 2 of the study was designed to supplement data from the Phase 1 study. Preliminary testing was done to select a new baseline composition from four formulations (BL1, BL2, BL3, and BL4). These were fabricated, heat treated, and analyzed for nepheline fraction. BL3 was the baseline glass composition selected for Phase 2 because it formed ~10 mass% nepheline during CCC heat treatment. BL3 was obtained by adjusting BL0 to increase Na_2O and reduce Li_2O (along with offsetting changes to other components).

A set of 13 glasses was then developed by adjusting Al_2O_3, B_2O_3, Li_2O, Na_2O, and SiO_2 OCAT from their values in the BL3 baseline composition, resulting in the fabrication of 14 unique glasses (including BL3). Table 3.1 lists the targeted component lower and upper bounds (mass fractions) that were chosen for investigation in Phase 2. Each OCAT change was offset by changes in the remaining components, keeping them in the same relative proportions as in the BL3 baseline glass. These calculations were performed using Equation (3.1).

The Glass IDs and targeted compositions of the Phase 2 glasses are listed in Table 3.2. The composition analysis results (Fox et al. 2016) indicated that glass NP2-High Na was likely misbatched. The composition of NP2-High Na adjusted for the misbatch is shown in Table 3.2 with an asterisk (NP2-High Na*). This adjusted composition was used for normalization of the PCT results and is recommended to be used for all future property-composition modeling efforts. Further details about the misbatch of NP2-High Na are discussed in Section 5.2.

3.3 Phase 3 Experimental Design

The results from Phase 2 provided information about the HLW glass composition region over which nepheline did and did not precipitate and composition effects on how much nepheline formed. The results suggested that the fraction of nepheline in the CCC glass was not easily represented by first-order composition effects (i.e., linear combinations of component concentrations). So, Phase 3 was designed to investigate the effects on nepheline precipitation of changing components two-components-at-a-time (2CAT) and three-components-at-a-time (3CAT). Table 3.1 lists the targeted component lower and upper bounds (mass fractions) that were chosen for investigation in Phase 3. Starting with the same baseline glass as used in Phase 2 (BL3), a 16-glass experimental design, consisting of 2CAT and 3CAT variations of Al_2O_3, B_2O_3, Li_2O, Na_2O, and SiO_2, was developed. The Glass IDs and targeted compositions of the Phase 3 glasses are listed in Table 3.2.

3.3.1 Generating 2CAT and 3CAT Glass Compositions

The first step in developing the 16-glass Phase 3 experimental design was to generate all possible combinations of components varied 2CAT and 3CAT within the Phase 3 lower and upper bounds in Table 3.1. The 2CAT changes for a given pair of components (i, j) are denoted (g_i, g_j) = (L_i, L_j), (L_i, U_j), (U_i, L_j), and (U_i, U_j). The 3CAT changes for given triple of components (i, j, k) are denoted (g_i, g_j, g_k) = (L_i, L_j, L_k), (L_i, L_j, U_k), (L_i, U_j, L_k), (L_i, U_j, U_k), (U_i, L_j, L_k), (U_i, L_j, U_k), (U_i, U_j, L_k), and (U_i, U_j, U_k). In this notation, the mass fractions of the i^{th} and j^{th} components (g_i, g_j) are each changed to the lower bound (L) or the upper bound (U) of a component, as listed in Table 3.1. These combinations of component lower

bounds and upper bounds can be considered as combinations of changes of the components from their baseline values. These 2CAT and 3CAT changes were offset by changes in the remaining components, keeping them in the same relative proportions as in the BL3 baseline glass.

The glass compositions from the 2CAT changes were calculated using

$$g_i = g_{Bi} + \Delta_i \qquad g_j = g_{Bj} + \Delta_j \qquad g_h = g_{Bh} - \frac{(\Delta_i + \Delta_j) g_{Bh}}{1 - (g_{Bi} + g_{Bj})} \quad h \neq i, j \tag{3.2}$$

where

g_i and g_j = mass fractions of the components changed 2CAT

g_{Bi} and g_{Bj} = mass fractions of these components in the BL3 baseline glass

Δ_i and Δ_j = changes in the two components from their baseline values ($g_i - g_{Bi}$ and $g_j - g_{Bj}$), which can be positive or negative

g_h = mass fraction of any h^{th} component not changed 2CAT (i.e., the i^{th} and j^{th} components)

g_{Bh} = mass fraction of the h^{th} component in the BL3 baseline glass that is different from the i^{th} and j^{th} components ($h \neq i, j$).

As an example, suppose that Component 1 was varied from its baseline value (g_{B1}) to its upper bound (U_1) and Component 2 was varied from its baseline value (g_{B2}) to its lower bound (L_2). Then $\Delta_1 = U_1 - g_{B1}$ and $\Delta_2 = L_2 - g_{B2}$, where Δ_1 is positive and Δ_2 is negative.

Similarly, the glass compositions from the 3CAT changes were calculated using

$$\begin{aligned} g_i &= g_{Bi} + \Delta_i \\ g_j &= g_{Bj} + \Delta_j \\ g_k &= g_{Bk} + \Delta_k \end{aligned} \qquad g_h = g_{Bh} - \frac{(\Delta_i + \Delta_j + \Delta_k) g_{Bh}}{1 - (g_{Bi} + g_{Bj} + g_{Bk})} \quad h \neq i, j, k \tag{3.3}$$

where

g_i, g_j, and g_k = mass fractions of the components changed 3CAT

g_{Bi}, g_{Bj}, and g_{Bk} = mass fractions of these components in the BL3 baseline glass

Δ_i, Δ_j, and Δ_k = changes in the three components from their baseline values ($g_i - g_{Bi}$, $g_j - g_{Bj}$, and $g_k - g_{Bk}$), which can be positive or negative

g_h = mass fraction of any h^{th} component not changed 3CAT (i.e., the i^{th}, j^{th}, and k^{th} components)

g_{Bh} = mass fraction of the h^{th} component in the BL3 baseline glass that is different from the i^{th}, j^{th}, and k^{th} components ($h \neq i, j, k$).

Calculating Δ_i, Δ_j, and Δ_k values for 3CAT variations is a natural extension of the previous illustration for calculating Δ_i and Δ_j values for 2CAT variations.

When applying the formulas in Equations (3.2) and (3.3) to calculate the 2CAT and 3CAT glass compositions, there were some 2CAT and 3CAT combinations of lower and/or upper bounds for which

the offsetting changes caused one or more of the remaining components to fall outside of their Phase 3 lower or upper bounds in Table 3.1. For example, the 2CAT combination with B_2O_3 and SiO_2 both at their upper bounds (0.22 and 0.33, respectively) led to a value of Al_2O_3 below its lower bound of 0.255. As another example, the 3CAT combination with Al_2O_3, B_2O_3, and SiO_2 all at their lower bounds caused both Li_2O and Na_2O to be above their upper bounds. It was decided that all varied components should remain within the lower and upper bounds specified for Phase 3 in Table 3.1. To achieve this, when necessary the combinations of components varied 2CAT and 3CAT were shrunk toward the BL3 baseline composition until all remaining components were within their lower and upper bounds after applying the offsetting changes. In such cases, the modified 2CAT and 3CAT changes led to (i) values of varied components above their lower bounds and below their upper bounds, and (ii) components other than those involved in the 2CAT or 3CAT changes being adjusted to their lower or upper bounds. This was judged acceptable, because of the limitations of varying five main components 2CAT and 3CAT with limited ranges of mass fractions of the remaining components used to offset the 2CAT and 3CAT changes. Ultimately, there were forty (40) 2CAT glass compositions and eighty (80) 3CAT glass compositions, for a total of 120 glass compositions that varied components 2CAT and 3CAT.

3.3.2 Selecting an Optimal Subset of 2CAT and 3CAT Compositions for the Phase 3 Study

An *optimal experimental design* approach (Atkinson et al. 2007) was chosen to optimally augment a set of 21 existing glass compositions with a set of 16 Phase 3 glasses selected from the set of 120 glasses with five main components varied 2CAT and 3CAT. The 21 existing glass compositions are listed in Table 3.3. The 21 existing glasses consisted of (i) three baseline compositions not tested in Phases 1 and 2 (BL1, BL2, and BL4) and (ii) a subset of 18 Phase 1 and Phase 2 glasses, all of which were within the Phase 3 glass composition region (specified by the lower and upper bounds listed in Table 3.1). The detection of Phase 2 glass "NP2-High Na" as being misbatched did not occur until after the Phase 3 experimental design was completed. Hence, the original targeted composition for that glass (see Tables 3.2 and 3.3) is the one that was used as an existing glass composition.

Optimality criteria for generating experimental designs depend on specifying a model form that is assumed to adequately represent the dependence of the response variable [fraction of nepheline in a glass (f_{Np}) in this application][1] to the predictor variables (glass composition in this application). The model form

$$f_{NP} = \sum_{i=1}^{5} b_i g_i + b_{\text{Rest}} g_{\text{Rest}} + \sum_{i=1}^{4} \sum_{j=i+1}^{5} b_{ij} g_i g_j + \sum_{i=1}^{3} \sum_{j=i+1}^{4} \sum_{k=j+1}^{5} b_{ijk} g_i g_j g_k + \sum_{i=1}^{4} \sum_{j=i+1}^{5} d_{ij} g_i g_j (g_i - g_j) \quad (3.4)$$

was assumed, where

[1] It is also of interest to predict whether or not nepheline precipitates, which is a binary response (yes or no). However, at the time this work was done, there were no statistical methods specifically for designing mixture experiments with a binary response variable. (Subsequently, a journal article on this topic has been published.) Hence, the experiment was designed focusing on a continuous response variable, the fraction of nepheline in a glass.

g_i, g_j, g_k	=	mass fraction of the i^{th}, j^{th}, *and* k^{th} glass component (i, j, k = 1, 2, 3, 4, 5 correspond to Al_2O_3, B_2O_3, Li_2O, Na_2O, and SiO_2)
g_{Rest}	=	mass fraction of the rest of the components making up the HLW glass composition
b_i, b_{Rest}	=	coefficients of the linear terms of the model associated with the components Al_2O_3, B_2O_3, Li_2O, Na_2O, SiO_2, and Rest
b_{ij}, b_{ijk}, d_{ij}	=	coefficients of crossproduct terms representing (i) quadratic-blending, (ii) special-cubic blending, and (iii) full-cubic blending effects of the components Al_2O_3, B_2O_3, Li_2O, Na_2O, and SiO_2 on the response variable (Cornell 2002).

Note that $\sum_{i=1}^{5} g_i + g_{Rest} = 1.0$, so that Equation (3.4) is a mixture experiment model (Cornell 2002). It was not necessarily expected that as complicated of a mixture experiment model form as given in Equation (3.4) will eventually be needed to represent the relationship between f_{Np} and glass composition. However, the model in Equation (3.4) was chosen as the basis for designing the Phase 3 experiment to provide support for exploring more complicated effects of glass composition on f_{Np}, if present.

Optimal experimental design uses an optimization algorithm that is not guaranteed to find the optimal design on any given run. Hence, the ACED optimal design software (Welch 1987) was used to perform 20 runs for each of three design optimality criteria associated with what are now commonly referred to as D-optimality, G-optimality, and I-optimality (Atkinson et al. 2007). Each run resulted in a set of sixteen 2CAT and/or 3CAT glass compositions with the goal of optimally augmenting the 21 existing glass compositions per a specific optimality criterion. See Welch (1987) and Welch (1984) for explanations of how the three criteria related to D-, G-, and I-optimality are defined and implemented in ACED. The 60 possible experimental designs (of 16 glass compositions) were narrowed down to four designs using several design optimality criteria to compare the 60 designs. The remaining four design options were compared graphically and using predictions of various glass properties from previously existing property-composition models (Vienna et al. 2009). The 16-glass experimental design ultimately selected consisted of eight 2CAT glasses and eight 3CAT glasses.

The Glass IDs and targeted glass compositions of the 16-glass Phase 3 experimental design are listed in Table 3.2. Figure 3.1 displays in a scatterplot matrix the targeted compositions of the Phase 3 glasses, along with the targeted compositions of four baseline glasses and the 17 Phase 1 and Phase 2 glasses that were within the Phase 3 glass composition region. The pairwise scatterplots show that the glass compositions provide good pairwise coverage of the Phase 3 region. The absence of points in the upper right portion of both the Na_2O-SiO_2 plot and the B_2O_3-SiO_2 plot means that those component combinations could not be at their upper bounds at the same time. Similarly, the absence of points in the lower left portion of the Al_2O_3-B_2O_3 plot means that those two components could not be at their lower bounds at the same time.

Table 3.3. Targeted Compositions (mass fractions) for the 21 Existing Glasses within the HLW Nepheline Phase 3 Composition Region

Glass ID	Phase	Al_2O_3	B_2O_3	Bi_2O_3	CaO	Cr_2O_3	F	Fe_2O_3	Li_2O	MnO	Na_2O	NiO	P_2O_5	RuO_2	SiO_2	SO_3	ZrO_2	Sum[a]
BL1	(b)	0.2900	0.1640	0.0070	0.0070	0.0100	0.0035	0.0250	0.0400	0.0100	0.1500	0.0000	0.0075	0.0005	0.2800	0.0025	0.0030	1.0000
BL2	(b)	0.2850	0.1700	0.0065	0.0065	0.0110	0.0030	0.0250	0.0400	0.0100	0.1405	0.0000	0.0070	0.0005	0.2900	0.0025	0.0025	1.0000
BL4	(b)	0.2850	0.1700	0.0065	0.0065	0.0110	0.0030	0.0250	0.0400	0.0100	0.1305	0.0000	0.0070	0.0005	0.3000	0.0025	0.0025	1.0000
Neph-NN-1-01[c][d]	1	0.2850	0.1800	0.0075	0.0050	0.0050	0.0000	0.0250	0.0600	0.0100	0.1000	0.0025	0.0100	0.0005	0.3070	0.0025	0.0000	1.0000
Neph-NN-1-02[d]	1	0.3000	0.1762	0.0073	0.0049	0.0049	0.0000	0.0245	0.0587	0.0098	0.0979	0.0024	0.0098	0.0005	0.3006	0.0024	0.0000	0.9999
Neph-NN-1-04[d]	1	0.2711	0.2200	0.0071	0.0048	0.0048	0.0000	0.0238	0.0571	0.0095	0.0951	0.0024	0.0095	0.0005	0.2920	0.0024	0.0000	1.0001
Neph-NN-1-07[d]	1	0.2764	0.1746	0.0073	0.0350	0.0048	0.0000	0.0242	0.0582	0.0097	0.0970	0.0024	0.0097	0.0005	0.2977	0.0024	0.0000	0.9999
Neph-NN-1-09[d]	1	0.2777	0.1754	0.0073	0.0049	0.0049	0.0000	0.0500	0.0585	0.0097	0.0974	0.0024	0.0097	0.0005	0.2991	0.0024	0.0000	0.9999
Neph-NN-1-12[d]	1	0.2692	0.1700	0.0071	0.0047	0.0047	0.0000	0.0236	0.0567	0.0094	0.1500	0.0024	0.0094	0.0005	0.2899	0.0024	0.0000	1.0000
Neph-NN-1-14[d]	1	0.2797	0.1766	0.0074	0.0049	0.0049	0.0000	0.0245	0.0589	0.0098	0.0981	0.0025	0.0098	0.0005	0.3200	0.0025	0.0000	1.0001
BL3	2	0.2850	0.1720	0.0065	0.0065	0.0110	0.0030	0.0250	0.0500	0.0100	0.1250	0.0000	0.0070	0.0005	0.2935	0.0025	0.0025	1.0000
NP2-High Al	2	0.3150	0.1648	0.0062	0.0062	0.0105	0.0029	0.0240	0.0479	0.0096	0.1198	0.0000	0.0067	0.0005	0.2812	0.0024	0.0024	1.0001
NP2-High B	2	0.2685	0.2200	0.0061	0.0061	0.0104	0.0028	0.0236	0.0471	0.0094	0.1178	0.0000	0.0066	0.0005	0.2765	0.0024	0.0024	1.0002
NP2-High Li	2	0.2820	0.1702	0.0064	0.0064	0.0109	0.0030	0.0247	0.0600	0.0099	0.1237	0.0000	0.0069	0.0005	0.2904	0.0025	0.0025	1.0000
NP2-High Na[e]	2	0.2752	0.1661	0.0063	0.0063	0.0106	0.0029	0.0241	0.0483	0.0097	0.1550	0.0000	0.0068	0.0005	0.2834	0.0024	0.0024	1.0000
NP2-High Na*[e]	2	0.2745	0.1657	0.0063	0.0063	0.0106	0.0029	0.0240	0.0482	0.0097	0.1546	0.0000	0.0068	0.0005	0.2827	0.0024	0.0048	1.0000
NP2-High Si	2	0.2703	0.1631	0.0062	0.0062	0.0104	0.0028	0.0237	0.0474	0.0095	0.1185	0.0000	0.0066	0.0005	0.3300	0.0024	0.0024	1.0000
NP2-Low Al	2	0.2550	0.1792	0.0068	0.0068	0.0115	0.0031	0.0260	0.0521	0.0104	0.1302	0.0000	0.0073	0.0005	0.3058	0.0026	0.0026	0.9999
NP2-Low B	2	0.2960	0.1400	0.0068	0.0068	0.0114	0.0031	0.0260	0.0519	0.0104	0.1298	0.0000	0.0073	0.0005	0.3048	0.0026	0.0026	1.0000
NP2-Low Li	2	0.2880	0.1738	0.0066	0.0066	0.0111	0.0030	0.0253	0.0400	0.0101	0.1263	0.0000	0.0071	0.0005	0.2966	0.0025	0.0025	1.0000
NP2-Low Na	2	0.2948	0.1779	0.0067	0.0067	0.0114	0.0031	0.0259	0.0517	0.0103	0.0950	0.0000	0.0072	0.0005	0.3036	0.0026	0.0026	1.0000
NP2-Low Si	2	0.2985	0.1802	0.0068	0.0068	0.0115	0.0031	0.0262	0.0524	0.0105	0.1309	0.0000	0.0073	0.0005	0.2600	0.0026	0.0026	0.9999

(a) The component mass fraction values were calculated to more decimal places and summed to unity. However, rounding to four decimal places for this table led to sums different from 1.0000 by ±0.0002.

(b) Baseline glasses tested outside of Phases 1 and 2. Two other baseline glasses, BL0 (Neph-NN-1-01) and BL3 were also tested, and were included in Phases 1 and 2, respectively.

(c) Neph-NN-1-01 is baseline glass BL0.

(d) These Phase 1 glasses varied components to min, mid, or max values: 01 = BL0, 02 = Max Al, 04 = Max B, 07 = Mid Ca, 09 = Min Fe, 12 = Max Na, and 14 = max Si.

(e) Glass NP2-High Na is the target composition originally selected for the Phase 2 experimental design and used as an "existing glass" composition to develop the Phase 3 experimental design. However, it was subsequently determined that the glass was misbatched, so the final adjusted composition is listed as NP2-High Na*. This is the composition recommended for modeling purposes.

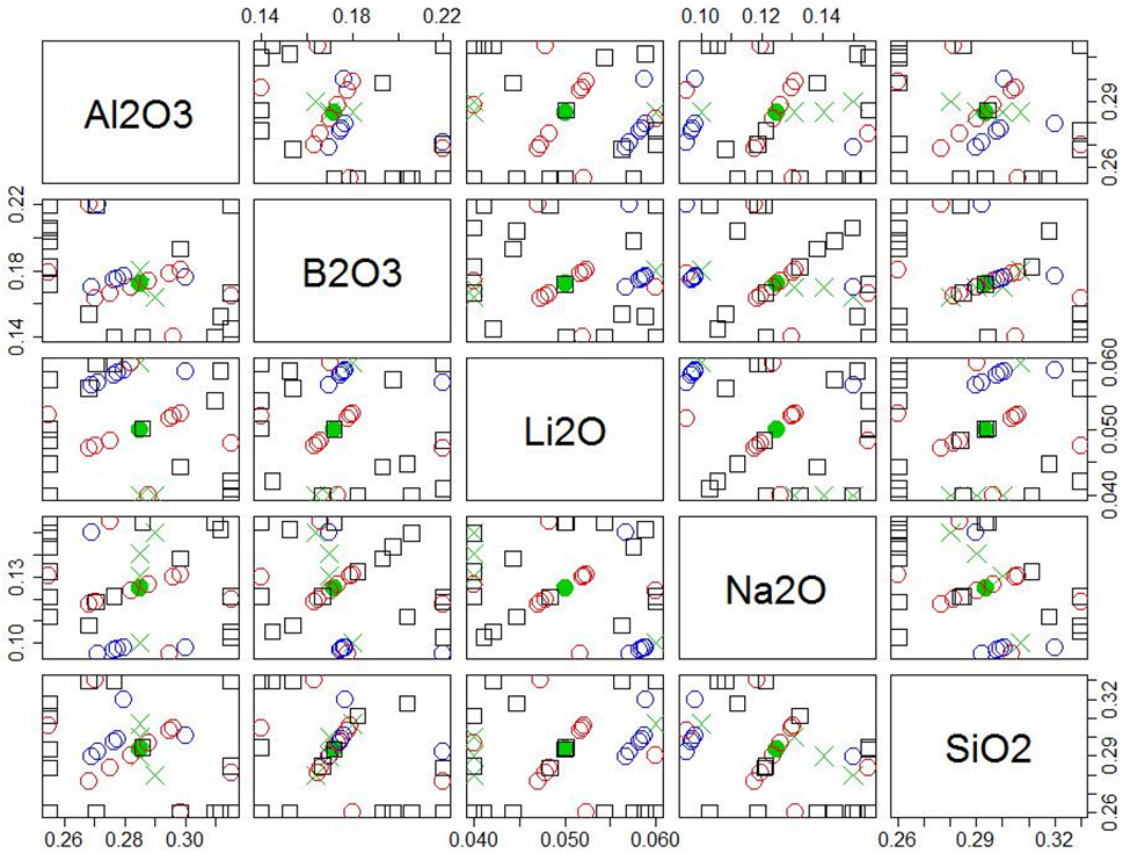

Figure 3.1. Scatterplot Matrix of Al_2O_3, B_2O_3, Li_2O, Na_2O, and SiO_2 Targeted Component Mass Fractions for the Phase 3 Glasses and the Phase 1 and Phase 2 Glasses Inside the Phase 3 Glass Composition Region (• = BL3 baseline glass, × = other baseline glasses, ○ = Seven Phase 1 glasses, ○ = 10 Phase 2 glasses, and □ = 16 Phase 3 glasses)

4.0 Experimental Methods

4.1 Glass Fabrication

For all phases, the simulated HLW glasses were prepared in 250 g or 300 g batches and melted in Pt-10% Rh crucibles. Oxides (Bi_2O_3, Cr_2O_3, Fe_2O_3, MnO, NiO, SiO_2, and ZrO_2) and carbonates ($CaCO_3$, Li_2CO_3, and Na_2CO_3) comprised most of the batching material. NaF, $NaPO_3$, and Na_2SO_4 were used as the sources of F, P_2O_5, and SO_3, respectively. Boric acid was used as the B_2O_3 source, and $Al(OH)_3$ was chosen as the aluminum additive. $RuNO(NO_3)_3$ was the source of RuO_2 in Phases 2 and 3, while RuO_2 was used in Phase 1.

For the glasses made with $RuNO(NO_3)_3$, 1.5% $RuNO(NO_3)_3$ solution was added dropwise to pre-weighed SiO_2 on a large watch glass and dried at 90°C for at least one hour before continuing with batching. After the appropriate amount of each source chemical was combined, the mixture was placed in an agate mill with an agate puck on a vibratory fixture for four minutes to obtain homogeneity. The batch was loaded into a Pt-10% Rh crucible in two to four separate additions that were allowed to melt down for ~10 minutes at the melt temperature (listed in Table 3.2) before the subsequent addition. Before the first addition, the furnace was preheated to the melt temperature. After the entire batch was added, a Pt-10% Rh lid was placed on the crucible and the melt was allowed to dwell for ~45 minutes. The melt was quenched by pouring onto a stainless steel plate. The glass was then ground in a tungsten carbide mill for four minutes and re-melted using the same melt process.

4.2 Canister Centerline Cooling Heat Treatment

To perform the CCC heat treatment, a crushed specimen of quenched glass was placed in either a 1.2 × 1.2 × 1.2 cm or a 2.54 × 2.54 × 2.54 cm Pt-10% Rh foil crucible with a tight-fitting lid. For the Phase 1 glasses, the glass-loaded crucibles were placed in a furnace preheated to 1050°C, allowed to dwell for 10 to 15 minutes, and then cooled in the furnace as prescribed in Table 4.1.

Table 4.1. CCC Heat Treatment Schedule

Start-Stop Temp (°C)	Rate (°C/hour)
1050-980	-93.3
980-930	-48.4
930-875	-35.5
875-825	-23.3
825-775	-15.2
775-725	-16.7
725-400	-18.2

This heat treatment is referred to as the WTP-1 CCC. For each glass in Phases 2 and 3, the glass-loaded crucible was placed in a furnace preheated to the respective melt temperature, and allowed to dwell for 30 minutes. Then, the furnace temperature was quickly reduced to 1050°C (at an estimated rate of -12.5°C/minute) before proceeding with the same cooling schedule as the Phase 1 glasses. This heat treatment is referred to as the WTP-2 CCC. When the furnace temperature was below 400°C (below the glass transition temperature), the furnace power was turned off and the glass was allowed to cool naturally to room temperature.

To prepare enough sample material for the PCT measurements (sub-sample IDs ending with "-CCC-PCT" in Table 5.1, which is discussed in Section 5.1), the quenched glass-loaded crucibles were placed in a furnace preheated to the glass melt temperature for ~5 minutes to allow the crushed glass to melt. Then, the crucible was removed from the furnace and additional pieces of quenched glass added before continuing with the heat treatment as described above.

4.3 X-Ray Diffraction Analysis

X-ray diffraction (XRD) was performed to identify and quantify the major crystalline phases in the CCC heat-treated samples and some of the quenched samples. For the CCC samples, either the entire heat-treated glass specimen was selected or it was cut diagonally through the center and half was used for analysis. These 1 to 3 g pieces were ground for ~15 s in a tungsten carbide mill, spiked with ~5.0 mass% of either a CaF_2 or a ZnO standard, and then milled for another ~45 s. The sub-sample IDs ending with -CCC-PCT or -Q-PCT in Table 5.1 (XRD results table, discussed in Section 5.1) were prepped for analysis from the excess (untested) fines returned from PCT sample preparation at Savannah River National Laboratory (SRNL) (Fox et al. 2016). The fines were spiked with ~5.0 mass% ZnO as a standard and then milled for ~45 s in a tungsten carbide mill. The powdered samples were then loaded into plastic holders and analyzed using a Bruker D8 Advance XRD (Bruker AXS Inc., Madison, Wisconsin) with Cu Kα emission. The detector used was a LynxEye™ position-sensitive detector with a collection window of 3° 2θ. Scan parameters were either 5 to 70° 2θ or 5 to 75° 2θ with a step of 0.015° 2θ and either 0.3 s or 0.6 s dwell at each step. Bruker AXS DIFFRACplus EVA software was used to identify the crystalline phases. TOPAS software was used to quantify the fractions of each phase using a whole-pattern fitting technique (Cheary et al. 2004).

4.4 Composition Analyses

Composition analysis was performed on all glasses from Phases 2 and 3, as well as the single WWFTP QA qualified Phase 1 glass (glass Neph-NN-1-12, see discussion in Section 2.2). The composition analyses of the study glasses were performed by Fox et al. (2016) and the procedure used is briefly summarized here.

A sample of the quenched version of each study glass was prepared in duplicate using two techniques: peroxide fusion (PF) and acid dissolution (AD). The PF method was selected for the analysis of major components, while the AD method was used for those components that could not be analyzed using the PF method due to interferences or low (minor) concentrations. The PF method is described in a SRNL procedure.[1] The AD method used concentrated nitric acid, hydrochloric acid, hydrofluoric acid, and saturated boric acid for digestion of finely crushed glass samples.

Fluorine concentrations were not measured because this would have required the use of an additional preparation method. Targeted fluorine concentrations were also low (~0.3 mass%) so they were likely to be near or below analytical detection limits. The concentrations of RuO_2 in these glasses were below detectable limits and were not included as part of the composition analyses. Each of the prepared samples was analyzed twice for the elements of interest using inductively coupled plasma–optical emission

[1] Savannah River National Laboratory. 2013. "Dissolution of Glass, Sludge, and Slurry Samples using Na_2O_2/NaOH/HCl." Manual L29, ITS-0040, Aiken, South Carolina.

spectroscopy (ICP-OES). Reference materials were also analyzed to ensure instrument accuracy. Further details on the composition analyses are reported by Fox et al. (2016).

4.5 Product Consistency Test

The PCT was conducted as described by Fox et al. (2016). PCT Method-A (ASTM 2014) was performed in triplicate on the quenched and CCC versions of each glass from Phases 2 and 3, as well as the single WWFTP QA qualified Phase 1 glass (glass Neph-NN-1-12, see discussion in Section 2.2). Approved Reference Material (ARM) glass and blanks were also run. Samples were ground, washed, and prepared according to the standard procedure. Fifteen milliliters of Type-I ASTM water were added to 1.5 g of glass in stainless steel vessels, which were then sealed and placed in a 90°C oven for seven days. After cooling, the solutions were filtered, acidified, and analyzed by ICP-OES. Multi-element standard solutions were also analyzed to ensure accuracy. The PCT releases of B, Li, Na, and Si were normalized to the targeted and measured compositions using the average of the measured leachate concentrations (over the triplicate results). Further details on the PCT work on these glasses are reported by Fox et al. (2016).

Only the PCT results (B, Li, Na, and Si releases) normalized using targeted glass compositions were used in the PNNL work described in this report. The experience at PNNL over many years using high-purity batching chemicals and careful weighing and melting procedures is that target glass compositions are generally more accurate representations of actual glass compositions than are analyzed glass compositions. This is because analyzed glass compositions are subject to varying magnitudes of uncertainty and can be subject to bias. The rare exception when a targeted composition is not the preferred representative of the actual glass composition is when a glass is misbatched, or when concentrations of volatile components are reduced during melting. In such cases, analyzed glass compositions are used to identify the misbatched component(s) or estimate the actual concentrations of volatile components, and then adjusted-targeted compositions are calculated.

5.0 Results

Including the single WWFTP QA qualified Phase 1 glass (glass Neph-NN-1-12, see discussion in Section 2.2) and all glasses from Phases 2 and 3, 31 new glass compositions were formulated, fabricated, analyzed for chemical composition, and CCC heat treated. The quenched and CCC versions of these glasses were evaluated for PCT response and analyzed for crystal fraction. Nepheline was identified in 24 CCC glasses. Eucryptite was identified in three CCC glasses, two of which also precipitated nepheline. The crystal fraction, PCT response, and composition analysis data are presented in this section. This section also contains results associated with the Phase 1 study, as well as the investigation of baseline compositions. The laboratory work associated with all Phase 1 glasses, except the single WWFTP QA qualified Phase 1 glass (Neph-NN-1-12), as well as baseline glasses BL1, BL2, and BL4 did not adhere to the WWFTP QA program (see Section 2.2); therefor these results are considered FIO.

5.1 X-Ray Diffraction Crystal Fraction Results

The quantitative XRD crystal fraction results for all glasses are summarized in Table 5.1. In Table 5.1 the sub-sample ID can be deciphered as the GlassID-CoolingProcess-AnalysisType-ReplicateNumber. If CCC heat treatment was performed for a specific sample, the CCC version (WTP-1 or WTP-2) is listed in the Heat Treatment column. The measured nepheline and eucryptite crystal fractions are listed in the "NP" and "EU" columns of Table 5.1, respectively, as well as the other major phases (≥1 mass%) identified. Baseline glasses BL1, BL2 and BL4 were not part of a particular phase of the study; this is indicated using a dash (-) in Table 5.1. If available, the Inorganic Crystal Structure Database (ICSD) collection codes (CC) for the crystalline phases identified in the sample are listed in the "CC" column of Table A.1 in Appendix A. That table also lists the CCC crucible size used for each sub-sample.

In Table 5.1, the sub-sample IDs ending with "-PCT" are powdered portions of the sample sent for PCT; these were prepared prior to beginning the PCT. XRD was performed on the quenched version of some glasses, these are identified by a "Q" in the sub-sample ID and heat treatment column. The CCC samples of glass NP-MC-AlBSi-1 had peaks on the XRD spectra for which an appropriate pattern in the ICSD could not be identified and fitting for quantification. The XRD spectrum of the sample with unfit peaks is shown in Appendix B.

Table 5.1. XRD Crystal Percentage Results in Mass%

Glass ID	Phase	Sub-Sample ID	Heat Treatment	NP[(a)]	EU[(b)]	Other Crystalline Species[(c)]
BL1[(d)]	-	BL1-CCC-XRD-1	WTP-1	45[(d)]	0[(d)]	Trevorite, 3.4[(d)]
BL2[(d)]	-	BL2-CCC-XRD-1	WTP-1	41[(d)]	0[(d)]	Trevorite, 3.6[(d)]
BL4[(d)]	-	BL4-CCC-XRD-1	WTP-1	26[(d)]	0[(d)]	Trevorite, 3.5[(d)]
Neph-NN-1-01[(d)(e)]	1	Neph-NN-1-01-CCC-XRD-1	WTP-1	0[(d)]	0[(d)]	Li-Fe-Mn-O, 3.9[(d)]
Neph-NN-1-02[(d)]	1	Neph-NN-1-02-CCC-XRD-1	WTP-1	0[(d)]	0[(d)]	Li-Fe-Mn-O, 3.4[(d)]
Neph-NN-1-03[(d)]	1	Neph-NN-1-03-CCC-XRD-1	WTP-1	0[(d)]	0[(d)]	Nichromite, 3.4[(d)]
		Neph-NN-1-03-CCC-XRD-2	WTP-1	0[(d)]	0[(d)]	Nichromite, 3.1[(d)]
Neph-NN-1-04[(d)]	1	Neph-NN-1-04-CCC-XRD-1	WTP-1	0[(d)]	0[(d)]	Nichromite, 8.4[(d)]

Table 5.1. XRD Crystal Percentage Results in Mass% (cont'd)

Glass ID	Phase	Sub-Sample ID	Heat Treatment	NP[a]	EU[b]	Other Crystalline Species[c]
Neph-NN-1-05[d]	1	Neph-NN-1-05-CCC-XRD-1	WTP-1	0[d]	0[d]	Nichromite, 4.1[d]
		Neph-NN-1-05-CCC-XRD-2	WTP-1	0[d]	0[d]	Nichromite, 3.7[d]
Neph-NN-1-06[d]	1	Neph-NN-1-06-CCC-XRD-1	WTP-1	0[d]	0[d]	Nichromite, 1.8[d]
		Neph-NN-1-06-CCC-XRD-2	WTP-1	0[d]	0[d]	Nichromite, 1.7[d]
Neph-NN-1-07[d]	1	Neph-NN-1-07-CCC-XRD-1	WTP-1	0[d]	0[d]	Trevorite, 2.4[d]
		Neph-NN-1-07-CCC-XRD-2	WTP-1	0[d]	0[d]	Trevorite, 2.3[d]
Neph-NN-1-08[d]	1	Neph-NN-1-08-CCC-XRD-1	WTP-1	0[d]	0[d]	Li-Fe-O, 2.7[d]
Neph-NN-1-09[d]	1	Neph-NN-1-09-CCC-XRD-1	WTP-1	0[d]	0[d]	Nichromite, 5.3[d]
Neph-NN-1-10[d]	1	Neph-NN-1-10-CCC-XRD-1	WTP-1	0[d]	0[d]	Nichromite, 4.7[d]
Neph-NN-1-11[d]	1	Neph-NN-1-11-CCC-XRD-1	WTP-1	0[d]	0[d]	Nichromite, 3.3[d] Al-Cr-B-O, 8.7[d]
Neph-NN-1-12	1	Neph-NN-1-12-CCC-XRD-1	WTP-1	55	0	Li-Fe-O, 2.8
		Neph-NN-1-12-CCC-XRD-2	WTP-1	56	0	Li-Fe-O, 2.2
		Neph-NN-1-12-CCC-PCT	WTP-2	67	0	Trevorite, 3.2 Li-Al-O, 1.1
		Neph-NN-1-12-Q-PCT	Q	0	0	None
Neph-NN-1-13[d]	1	Neph-NN-1-13-CCC-XRD-1	WTP-1	0[d]	0[d]	Li-Fe-Mn-O, 6.2[d]
Neph-NN-1-14[d]	1	Neph-NN-1-14-CCC-XRD-1	WTP-1	0[d]	0[d]	Li-Fe-Mn-O, 5.5[d]
Neph-NN-1-15[d]	1	Neph-NN-1-15-CCC-XRD-1	WTP-1	0[d]	0[d]	Li-Fe-O, 1.7[d] Li-Fe-Cr-O, 2.0[d]
BL3	2	BL3-CCC-XRD-1	WTP-2	12	0	Li-Fe-O, 1.7 Li-Fe-Mn-O, 2.0
		BL3-CCC-XRD-2	WTP-2	14	0	Li-Fe-O, 2.3 Li-Fe-Mn-O, 1.6
		BL3-CCC-PCT	WTP-2	16	0	Li-Fe-O, 2.1 Li-Fe-Mn-O, 2.2
		BL3-Q-PCT	Q	0	0	Li-Fe-Mn-O, 2.8
NP2-High Al	2	NP2-HighAl-CCC-XRD-1	WTP-2	9.0	0	Li-Fe-Mn-O, 2.3 Li-Fe-Cr-O, 2.5
		NP2-HighAl-CCC-XRD-2	WTP-2	9.3	0	Li-Fe-Mn-O, 2.4 Li-Fe-Cr-O, 2.3
		NP2-HighAl-CCC-PCT	WTP-2	11	0	Li-Fe-Mn-O, 6.4
NP2-High B	2	NP2-HighB-CCC-XRD-1	WTP-2	1.0	0	Li-Fe-O, 2.9
		NP2-HighB-CCC-PCT	WTP-2	0.48	0	Li-Fe-O, 3.6
NP2-High Li	2	NP2-HighLi-CCC-XRD-1	WTP-2	44	0	Li-Fe-Mn-O, 2.1 Iron Oxide, 1.6
		NP2-HighLi-CCC-PCT	WTP-2	53	0	Li-Fe-Mn-O, 2.5 Iron Oxide, 1.9

Table 5.1. XRD Crystal Percentage Results in Mass% (cont'd)

Glass ID	Phase	Sub-Sample ID	Heat Treatment	NP[a]	EU[b]	Other Crystalline Species[c]
NP2-High Na	2	NP2-HighNa-CCC-XRD-1	WTP-2	56	0	Iron Oxide, 3.1
		NP2-HighNa-CCC-PCT	WTP-2	64	0	Li-Fe-O, 1.8
						Li-Fe-Mn-O, 2.3
NP2-High Si	2	NP2-HighSi-CCC-XRD-1	WTP-2	29	0	Li-Fe-O, 1.7
						Li-Fe-Mn-O, 1.4
		NP2-HighSi-CCC-XRD-2	WTP-2	29	0	Li-Fe-O, 2.0
						Li-Fe-Mn-O, 1.1
		NP2-HighSi-CCC-PCT	WTP-2	32	0	Li-Fe-O, 3.2
						Li-Fe-Mn-O, 1.3
NP2-Low Al	2	NP2-LowAl-CCC-XRD-1	WTP-2	4.0	0	Li-Fe-Mn-O, 3.1
		NP2-LowAl-CCC-PCT	WTP-2	6.2	0	Li-Fe-Mn-O, 3.5
NP2-Low B	2	NP2-LowB-CCC-XRD-1	WTP-2	60	0	Iron Oxide, 3.2
						Li-Fe-Mn-O, 1.0
		NP2-LowB-CCC-XRD-2	WTP-2	57	0	Iron Oxide, 3.0
						Li-Fe-Mn-O, 1.1
		NP2-LowB-CCC-PCT	WTP-2	66	0	Li-Fe-O, 4.0
NP2-Low Li	2	NP2-LowLi-CCC-XRD-1	WTP-2	1.8	0	Li-Fe-O, 2.6
						Li-Fe-Mn-O, 1.1
		NP2-LowLi-CCC-PCT	WTP-2	2.2	0	Li-Fe-O, 2.9
						Li-Fe-Mn-O, 1.2
NP2-Low Na	2	NP2-LowNa-CCC-XRD-1	WTP-2	0	8.7	Li-Fe-Mn-O, 3.9
		NP2-LowNa-CCC-PCT	WTP-2	0	5.9	Li-Fe-Mn-O, 5.3
		NP2-LowNa-Q-PCT	Q	0	0	Fe-Si-O, 2.1
						Eskolaite, 1.4
NP2-Low Si	2	NP2-LowSi-CCC-XRD-1	WTP-2	5.0	0	Li-Fe-Mn-O, 3.6
		NP2-LowSi-CCC-PCT	WTP-2	5.1	0	Li-Fe-Mn-O, 1.2
						Iron Oxide, 3.4
NP2-Very High Al	2	NP2-VeryHighAl-CCC-XRD-1	WTP-2	29	0	Al-O, 13
		NP2-VeryHighAl-CCC-PCT	WTP-2	36	0	Al-O, 16
						Iron Oxide, 1.1
NP2-Very High Si	2	NP2-VeryHighSi-CCC-XRD-1	WTP-2	0	0	Chromite, 2.0
		NP2-VeryHighSi-CCC-PCT	WTP-2	0	0	Chromite, 2.3
NP2-Very Low Si	2	NP2-VeryLowSi-CCC-XRD-1	WTP-2	23	0	Li-Fe-Mn-O, 1.5
						Li-Fe-Cr-O, 4.0
		NP2-VeryLowSi-CCC-PCT	WTP-2	37	0	Li-Fe-Mn-O, 8.0
		NP2-VeryLowSi-Q-PCT	Q	0	0	Li-Fe-Cr-O, 4.0

Table 5.1. XRD Crystal Percentage Results in Mass% (cont'd)

Glass ID	Phase	Sub-Sample ID	Heat Treatment	NP[(a)]	EU[(b)]	Other Crystalline Species[(c)]
NP-MC-AlB-1	3	NP-MC-AlB-1-CCC-XRD-1	WTP-2	0	0	Li-Fe-Mn-O, 3.2
		NP-MC-AlB-1-CCC-XRD-2	WTP-2	0	0	Li-Fe-Mn-O, 3.3
		NP-MC-AlB-1-CCC-PCT	WTP-2	0	0	Li-Fe-Mn-O, 3.3
NP-MC-AlBNa-1	3	NP-MC-AlBNa-1-CCC-XRD-1	WTP-2	0	0	Li-Fe-O, 2.1 Li-Fe-Mn-O, 1.6
		NP-MC-AlBNa-1-CCC-PCT	WTP-2	0	0	Li-Fe-O, 2.0 Li-Fe-Mn-O, 1.9
NP-MC-AlBNa-2	3	NP-MC-AlBNa-2-CCC-XRD-1	WTP-2	5.2	0	Iron Oxide, 2.5 Li-Fe-Mn-O, 1.1
		NP-MC-AlBNa-2-CCC-PCT	WTP-2	4.9	0	Li-Fe-Mn-O, 2.5 Iron Oxide, 1.1
NP-MC-AlBSi-1	3	NP-MC-AlBSi-1-CCC-XRD-1	WTP-2	0	0	Fe-Cr-O, 1.4 Na-Al-O, 1.9
		NP-MC-AlBSi-1-CCC-PCT	WTP-2	0	0	Fe-Cr-O, 1.2 Na-Al-O, 1.7
		NP-MC-AlBSi-1-Q-PCT	Q	0	0	None
NP-MC-AlLi-1	3	NP-MC-AlLi-1-CCC-XRD-1	WTP-2	0.77	0	Fe-Si-O, 3.2
		NP-MC-AlLi-1-CCC-PCT	WTP-2	0.94	0	Iron Oxide, 2.8
NP-MC-AlLi-2	3	NP-MC-AlLi-2-CCC-XRD-1	WTP-2	35	0	Li-Fe-O, 1.7
		NP-MC-AlLi-2-CCC-XRD-2	WTP-2	39	0	Li-Fe-O, 3.3
		NP-MC-AlLi-2-CCC-PCT	WTP-2	38	0	Li-Fe-Mn-O, 4.5
		NP-MC-AlLi-2-Q-PCT	Q	0	0	Fe-Si-O, 2.7
NP-MC-AlLiNa-1	3	NP-MC-AlLiNa-1-CCC-XRD-1	WTP-2	61	0	Li-Fe-Mn-O, 5.0 Li-Al-B-O, 9.6
		NP-MC-AlLiNa-1-CCC-XRD-2	WTP-2	63	0	Li-Fe-Mn-O, 5.2 Li-Al-B-O, 12
		NP-MC-AlLiNa-1-CCC-PCT	WTP-2	66	0	Li-Fe-Mn-O, 5.1 Li-Al-B-O, 11
NP-MC-AlLiSi-1	3	NP-MC-AlLiSi-1-CCC-XRD-1	WTP-2	4.7	0	Li-Fe-Mn-O, 1.2 Fe-Si-O, 2.5
		NP-MC-AlLiSi-1-CCC-XRD-2	WTP-2	5.3	0	Li-Fe-Mn-O, 1.7 Fe-Si-O, 2.5
		NP-MC-AlLiSi-1-CCC-PCT	WTP-2	7.0	0	Li-Fe-Mn-O, 1.8 Fe-Si-O, 2.6

Table 5.1. XRD Crystal Percentage Results in Mass% (cont'd)

Glass ID	Phase	Sub-Sample ID	Heat Treatment	NP[(a)]	EU[(b)]	Other Crystalline Species[(c)]
NP-MC-AlNa-1	3	NP-MC-AlNa-1-CCC-XRD-1	WTP-2	57	0	Li-Fe-Mn-O, 1.1 Iron Oxide, 2.1 Nosean, 1.3
		NP-MC-AlNa-1-CCC-XRD-2	WTP-2	64	0	Li-Fe-Mn-O, 2.9 Iron Oxide, 1.2 Nosean, 1.6
		NP-MC-AlNa-1-CCC-PCT	WTP-2	69	0	Li-Fe-Mn-O, 3.4 Iron Oxide, 1.1
NP-MC-AlSi-1	3	NP-MC-AlSi-1-CCC-XRD-1	WTP-2	51	0	Li-Fe-O, 3.3 Li-Fe-Mn-O, 1.6
		NP-MC-AlSi-1-CCC-XRD-2	WTP-2	54	0	Li-Fe-O, 3.4 Li-Fe-Mn-O, 1.5
		NP-MC-AlSi-1-CCC-PCT	WTP-2	57	0	Li-Fe-O, 3.3 Li-Fe-Mn-O, 1.5
NP-MC-AlSi-2	3	NP-MC-AlSi-2-CCC-XRD-1	WTP-2	8.9	13	Fe-Cr-O, 1.3 Eskolaite, 1.1 Al-Cr-O, 1.2
		NP-MC-AlSi-2-CCC-XRD-2	WTP-2	9.5	14	Fe-Cr-O, 1.3 Eskolaite, 1.2
		NP-MC-AlSi-2-CCC-PCT	WTP-2	11	14	Fe-Cr-O, 1.4 Eskolaite, 1.4 Al-Cr-O, 1.7
NP-MC-BLiSi-1	3	NP-MC-BLiSi-1-CCC-XRD-1	WTP-2	59	5.2	Li-Fe-Mn-O, 2.9 Iron Oxide, 1.2 Silicon Oxide, 1.1
		NP-MC-BLiSi-1-CCC-PCT	WTP-2	63	7.9	Li-Fe-O, 1.7 Li-Fe-Mn-O, 2.1
		NP-MC-BLiSi-1-Q-PCT	Q	0	0	Li-Fe-Mn-O, 2.7
NP-MC-BLiSi-2	3	NP-MC-BLiSi-2-CCC-XRD-1	WTP-2	0	0	Li-Fe-Mn-O, 2.1 Iron Oxide, 1.2
		NP-MC-BLiSi-2-CCC-PCT	WTP-2	0	0	Li-Fe-Mn-O, 2.3 Iron Oxide, 1.0
NP-MC-BNa-1	3	NP-MC-BNa-1-CCC-XRD-1	WTP-2	67	0	Li-Fe-O, 2.9 Li-Fe-Mn-O, 1.3
		NP-MC-BNa-1-CCC-PCT	WTP-2	68	0	Li-Fe-O, 2.8 Li-Fe-Mn-O, 1.7
		NP-MC-BNa-1-Q-PCT	Q	3.1	0	Li-Fe-Mn-O, 1.8 Iron Oxide, 1.1

Table 5.1. XRD Crystal Percentage Results in Mass% (cont'd)

Glass ID	Phase	Sub-Sample ID	Heat Treatment	NP[(a)]	EU[(b)]	Other Crystalline Species[(c)]
NP-MC-BNaSi-1	3	NP-MC-BNaSi-1-CCC-XRD-1	WTP-2	55	0	Li-Fe-Mn-O, 7.2
		NP-MC-BNaSi-1-CCC-PCT	WTP-2	62	0	Li-Fe-Mn-O, 1.6
						Iron Oxide, 4.1
NP-MC-BSi-1	3	NP-MC-BSi-1-CCC-XRD-1	WTP-2	0	0	Eskolaite, 1.2
		NP-MC-BSi-1-CCC-PCT	WTP-2	0	0	Iron Oxide, 1.4

(a) NP = Nepheline
(b) EU = Eucryptite
(c) Some crystalline phases are abbreviated by symbols of the contained elements. Li-Fe-Mn-O, Li-Fe-O, Li-Fe-Cr-O, Fe-Si-O, and Al-O phases have spinel structure.
(d) Data are considered FIO
(e) Neph-NN-1-01 is BL0

5.2 Composition Analysis Results

The targeted and average measured component concentrations (mass%) in the quenched study glasses are presented in Appendix C. The composition analyses of glass samples were performed as described in Section 4.4.

The results presented in this section were summarized from the report by Fox et al. (2016). That report did not perform any statistical comparisons of targeted and analyzed values of glass components, as has traditionally been performed at PNNL. Using results of standard glasses analyzed with the glasses of interest, statistical analyses could have been performed to assess whether the analyzed glass composition results have statistically significant biases. If so, then bias-correction methods could have been applied to the analyzed glass compositions. Then, as discussed by Weier and Piepel (2003), the bias-corrected (if needed) analyzed glass compositions could have been normalized to sum to a total mass fraction of 1.0 (or a total mass percentage of 100). As Weier and Piepel (2003) discussed, normalized (after bias correction if needed) glass compositions have smaller uncertainties than unnormalized (and not bias-corrected) analyzed glass compositions. Also, statistical analyses could have been performed to assess whether differences in targeted and analyzed compositions are statistically different from zero, after accounting for analytical uncertainties (which can be different for different glass components). Appendix A of Hrma et al. (1994) illustrates this latter kind of statistical analysis.

The following observations are summarized from observations made in the Fox et al. (2016) report. Because Fox et al. (2016) did not perform any statistical analyses as discussed in the preceding paragraph, it is not clear whether some of the differences between targeted and analyzed glass compositions are (i) due to analytical bias, or (ii) within the uncertainties of analyzing the glass components. Typically, different glass components can have different analytical uncertainties. Because the analyzed glass composition data provided by Fox et al. (2016) were only used to assess whether the glasses were misbatched or were subject to component volatility, the lack of statistical analyses is not a critical shortcoming. Plots of the measured oxide values and measured versus targeted compositions in Exhibit A-2 and Exhibit A-4 of Fox et al. (2016) were considered. Still, appropriate caution should be exercised in evaluating the following observations adapted from Fox et al. (2016), since the differences mentioned may be a result of analytical bias or within analytical uncertainties.

- The measured Bi_2O_3 concentrations of the study glasses are generally low by about 10% relative, although the targeted concentrations of this oxide are less than 1 mass%.
- The measured CaO concentrations of the study glasses are generally lower than the targeted values, although the targeted concentrations of this oxide are less than 1 mass%.
- The measured Na_2O values appeared to be biased somewhat high.
- Measurements of ZrO_2 in glass NP2-High Na are consistently above the targeted value by about a factor of two. This component may have been inadvertently double batched in this glass.[1]
- All of the sums of the average measured oxides fall within the interval of 98 to 101 mass%, indicating recovery of all analyzed components (although F and RuO_2 were not analyzed as discussed in Section 4.4). Additionally, the relative difference between the measured and targeted values does not exceed 10% for any oxides with targeted values above 5 mass%.

Of the observations noted above, only the next-to-last one required an adjustment of the data. The targeted concentration of ZrO_2 in glass NP2-High Na was 0.24 mass%; however, all measurements of ZrO_2 in this glass were ~0.46 mass% (see Appendix C). In addition, a review of the glass batch sheets showed that most batch masses differed from the targeted batch mass by roughly -0.03% (relative), but NP2-High Na differed by 0.07% indicating that a minor component was likely added twice. From these observations it was determined that there is a high likelihood that ZrO_2 was added twice. An adjustment of the targeted composition of NP2-High Na (denoted as NP2-High Na* in Table 3.2) was determined by doubling the targeted ZrO_2 concentration (to 0.48 mass%) and renormalizing the composition. The adjusted composition, NP2-High Na*, was used for normalization of the PCT results and is recommended to be used in future modeling efforts.

The plots of measured oxide concentrations and measured versus targeted oxide concentrations in Exhibit A-2 and Exhibit A-4 of the Fox et al. (2016) report were considered to assess whether any components volatilized. In these plots, the data points associated with the measured SO_3 concentrations were observed to be somewhat scattered. Some SO_3 volatilization is likely, but the scatter in the measured values makes it difficult to quantify. Other than this observation, there was no indication of significant volatilization.

5.3 Product Consistency Test Results

The PCT was performed for all of the Phase 2 and Phase 3 glasses, but only for the single Phase 1 glass that formed nepheline (glass Neph-NN-1-12). Glass samples for PCT were prepared as described previously in Section 4.5. The releases of B, Li, Na, and Si were normalized using targeted compositions (denoted NC_B, NC_{Li}, NC_{Na}, and NC_{Si}) for the quenched and CCC samples. The normalized PCT releases are presented in Table 5.2.

The following observations were noted upon review of the PCT results (Fox et al. 2016).

- The quenched versions of all of the study glasses tested (i.e., all Phase 2 and Phase 3 glasses, and the one Phase 1 glass) have NC_B values that are well below the EA benchmark NC_B value of 16.695 g/L (Jantzen et al. 1993).

[1] The possible misbatch of NP2-High Na is documented in EWG-CAR-O3670.

- Many of the study glasses have higher NC_B, NC_{Li}, NC_{Na} values after the CCC heat treatment.
- NC_B, NC_{Li}, NC_{Na}, and NC_{Si} values for glasses NP2-High-B, NP2-Very-High-Si, NP-MC-AlB-1, NP-MC-AlBNa-1, and NP-MC-BSi-1 were relatively unaffected by the CCC heat treatment, and had NC_B values below the EA benchmark.
- Several glasses (NP2-Low-Al, NP2-Low-Li, NP2-Low-Na, NP2-Low-Si, NP-MC-AlBNa-2, NP-MC-AlBSi-1, NP-MC-AlLi-1, NP-MC-AlLiSi-1, NP-MC-AlSi-2, and NP-MC-BLiSi-2) had significant increases in NC_B, NC_{Li}, and NC_{Na} values after the CCC heat treatment.

Table 5.2. PCT Results for Quenched and CCC Glasses Normalized to the Targeted Compositions

Glass ID	Phase	Normalized PCT_Q[(a)] (g/L)				Normalized PCT_{CCC}[(b)] (g/L)			
		B	Li	Na	Si	B	Li	Na	Si
Neph-NN-1-12	1	2.539	2.133	1.732	0.498	83.965	64.550	16.176	0.087
BL3	2	1.830	1.777	1.156	0.505	22.974	13.396	7.735	0.159
NP2-High Al	2	1.984	1.952	1.224	0.434	17.574	8.689	7.051	0.159
NP2-High B	2	3.512	3.385	2.276	0.369	4.147	3.651	2.403	0.391
NP2-High Li	2	1.984	1.826	1.270	0.514	71.251	50.354	14.099	0.087
NP2-High Na*[(c)]	2	2.417	2.022	1.666	0.435	79.456	64.767	19.280	0.079
NP2-High Si	2	0.928	1.088	0.598	0.518	39.147	26.010	8.897	0.163
NP2-Low Al	2	2.208	1.984	1.335	0.483	7.776	5.597	2.485	0.226
NP2-Low B	2	1.434	1.447	0.961	0.539	81.649	58.199	12.379	0.072
NP2-Low Li	2	1.622	1.671	1.007	0.502	3.509	2.410	1.605	0.278
NP2-Low Na	2	1.235	1.429	0.696	0.556	4.384	2.949	1.932	0.335
NP2-Low Si	2	3.081	2.811	2.128	0.337	9.855	5.928	4.834	0.020
NP2-Very High Al	2	2.300	2.115	1.394	0.401	41.979	24.597	13.349	0.162
NP2-Very High Si	2	0.593	0.882	0.328	0.473	0.712	0.823	0.365	0.447
NP2-Very Low Si	2	15.382	8.942	12.671	0.100	53.596	39.828	27.400	0.038
NP-MC-AlB-1	3	4.137	3.711	2.446	0.379	3.966	3.385	2.298	0.337
NP-MC-AlBNa-1	3	0.877	1.064	0.571	0.546	1.344	1.149	0.662	0.631
NP-MC-AlBNa-2	3	3.479	3.101	2.399	0.313	12.092	7.508	6.682	0.034
NP-MC-AlBSi-1	3	2.675	2.648	1.723	0.381	3.634	3.122	2.340	0.026
NP-MC-AlLi-1	3	1.895	1.767	1.142	0.438	2.701	2.063	1.226	0.439
NP-MC-AlLi-2	3	1.582	1.683	1.009	0.406	20.848	12.377	6.943	0.200
NP-MC-AlLiNa-1	3	2.896	2.465	2.127	0.427	75.117	53.718	24.384	0.035
NP-MC-AlLiSi-1	3	4.333	3.767	2.967	0.273	14.128	9.270	6.863	0.185
NP-MC-AlNa-1	3	2.682	2.237	1.811	0.426	91.957	74.120	18.684	0.120
NP-MC-AlSi-1	3	4.227	3.692	2.926	0.375	80.339	63.856	22.808	0.115
NP-MC-AlSi-2	3	0.816	1.253	0.437	0.494	12.728	5.290	4.793	0.024
NP-MC-BLiSi-1	3	0.994	1.084	0.682	0.554	86.474	53.080	10.328	0.113
NP-MC-BLiSi-2	3	5.082	4.377	3.204	0.327	6.602	5.439	3.729	0.315
NP-MC-BNa-1	3	2.439	1.909	1.493	0.411	80.720	63.211	14.926	0.056
NP-MC-BNaSi-1	3	2.871	2.424	2.179	0.392	74.346	52.177	24.155	0.034
NP-MC-BSi-1	3	2.525	2.341	1.321	0.408	2.156	1.906	1.169	0.410

(a) PCT_Q = Product Consistency Test results for quenched glasses

(b) PCT_{CCC} = Product Consistency Test results for canister centerline cooled glasses

(c) The composition of NP2-High Na was adjusted for being misbatched, with the adjusted composition denoted NP2-High Na*. The PCT results were normalized to the adjusted composition.

6.0 Discussion and Conclusions

The Phase 2 study was developed to supplement the Phase 1 data. The baseline glass for the Phase 2 study (BL3) increased the concentration of Na_2O at the expense of Li_2O when compared to the targeted Phase 1 baseline composition (BL0). BL3 was also used as the baseline in the Phase 3 study. Twenty three of the 29 Phase 2 and 3 glasses formulated from BL3 formed nepheline during CCC heat treatment.

It is interesting to note that the -CCC-PCT results consistently show higher nepheline fractions than the -CCC-XRD results (see Table 5.1). The cause of this finding is not known, but slight differences between three experimental parameters could explain this trend: (i) loading of quenched glass into the CCC crucible, (ii) size of the CCC crucible, and (iii) XRD sample preparation. When preparing a CCC sample for PCT analysis, quenched glass was loaded into the CCC crucible in two additions to ensure enough sample was available for PCT measurements (see discussion in Section 4.2). For the same reason, all of the -CCC-PCT samples were heat treated in larger crucibles (see crucible size in Table A.1). This could allow the glass in the center of the larger CCC crucibles to cool slower as compared to the smaller CCC crucibles, allowing more time for crystallization to occur. Lastly, the XRD samples of these specimens were prepared from the sieved fines returned from PCT sample preparation, rather than solid glass samples (see Section 4.3).

The initial quantitative XRD crystal fraction results (sub-samples ending with -CCC-XRD-1) for the nepheline mass fractions in all 14 Phase 2 glasses are plotted against the differences in component mass fractions from the baseline glass (BL3) in Figure 6.1.

The single Phase 2 composition that formed eucryptite (NP2-Low Na) is plotted in Figure 6.1 with and without eucryptite (EU). In the Phase 2 study, the measured nepheline fractions of the initial eleven glasses (BL3, NP2-High Al, NP2-High B, NP2-High Li, NP2-High Na, NP2-High Si, NP2-Low Al, NP2-Low B, NP2-Low Li, NP2-Low Na, and NP2-Low Si) didn't follow expected trends. It was expected that increasing SiO_2 would decrease the nepheline fraction and increasing Al_2O_3 would increase the fraction of nepheline, but the opposites of these expectations were observed. For this reason, three additional compositions (NP2-Very Low Si, NP2-Very High Si, and NP2-Very High Al) were formulated. The data points for the three additional compositions are circled in red in Figure 6.1. From Figure 6.1, it is apparent that the composition region for which nepheline precipitated and the concentration of nepheline formed cannot be easily described by first-order composition effects. It was observed that increasing B_2O_3 concentration is the most effective method for suppressing nepheline formation and increasing alkali concentration promotes it. The impacts of SiO_2 and Al_2O_3 are more complicated.

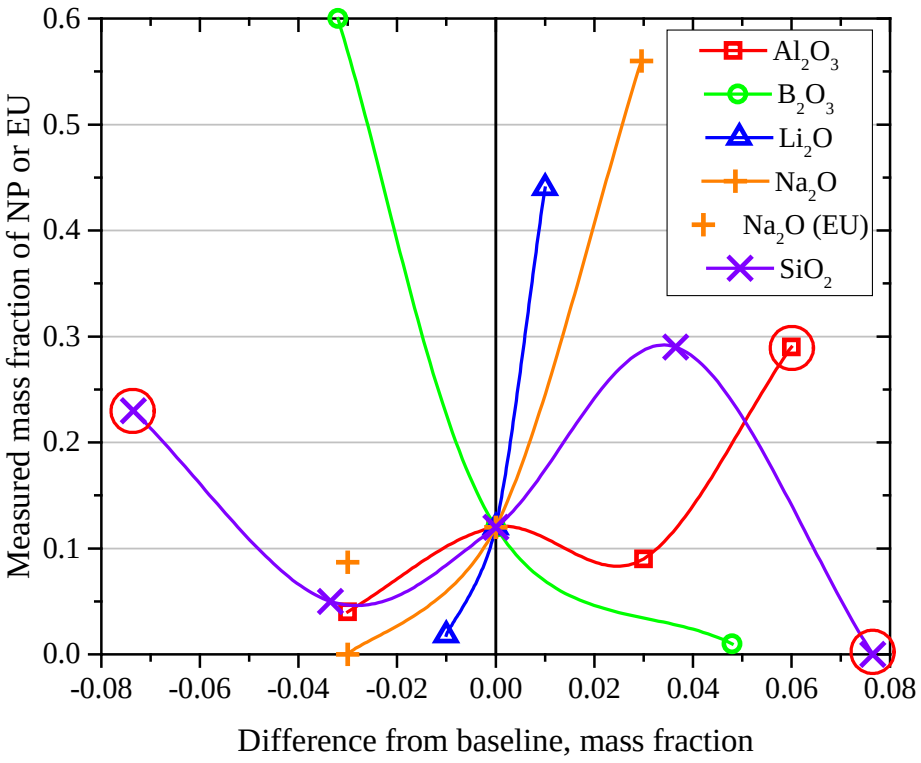

Figure 6.1. Measured Mass Fractions of Nepheline and Eucryptite in Glasses vs. Component Differences from the BL3 Baseline Glass (EU = Eucryptite, red circles indicate additional compositions)

The measured nepheline (NP) and eucryptite (EU) fractions are plotted against the PCT response for each CCC glass in Figure 6.2. All the quantitative XRD data presented in Table 5.1 are plotted in Figure 6.2. Each data point can be related back to Table 5.1 by the end of the sub-sample ID (shown in the legends of Figure 6.2). All glasses that precipitated only nepheline are plotted in blue, the glass with only eucryptite is plotted in red, and glasses that formed nepheline and eucryptite are plotted in green. These plots indicate a correlation between nepheline fraction and PCT responses. Generally, as the fraction of nepheline and eucryptite increases the normalized releases of B, Li, and Na increase. Normalized releases of Na are generally lower and more scattered than that of B and Li. This is likely observed because nepheline is a Na-containing crystal. As the fraction of nepheline increases, the fraction of Na in glass available for leaching is reduced.

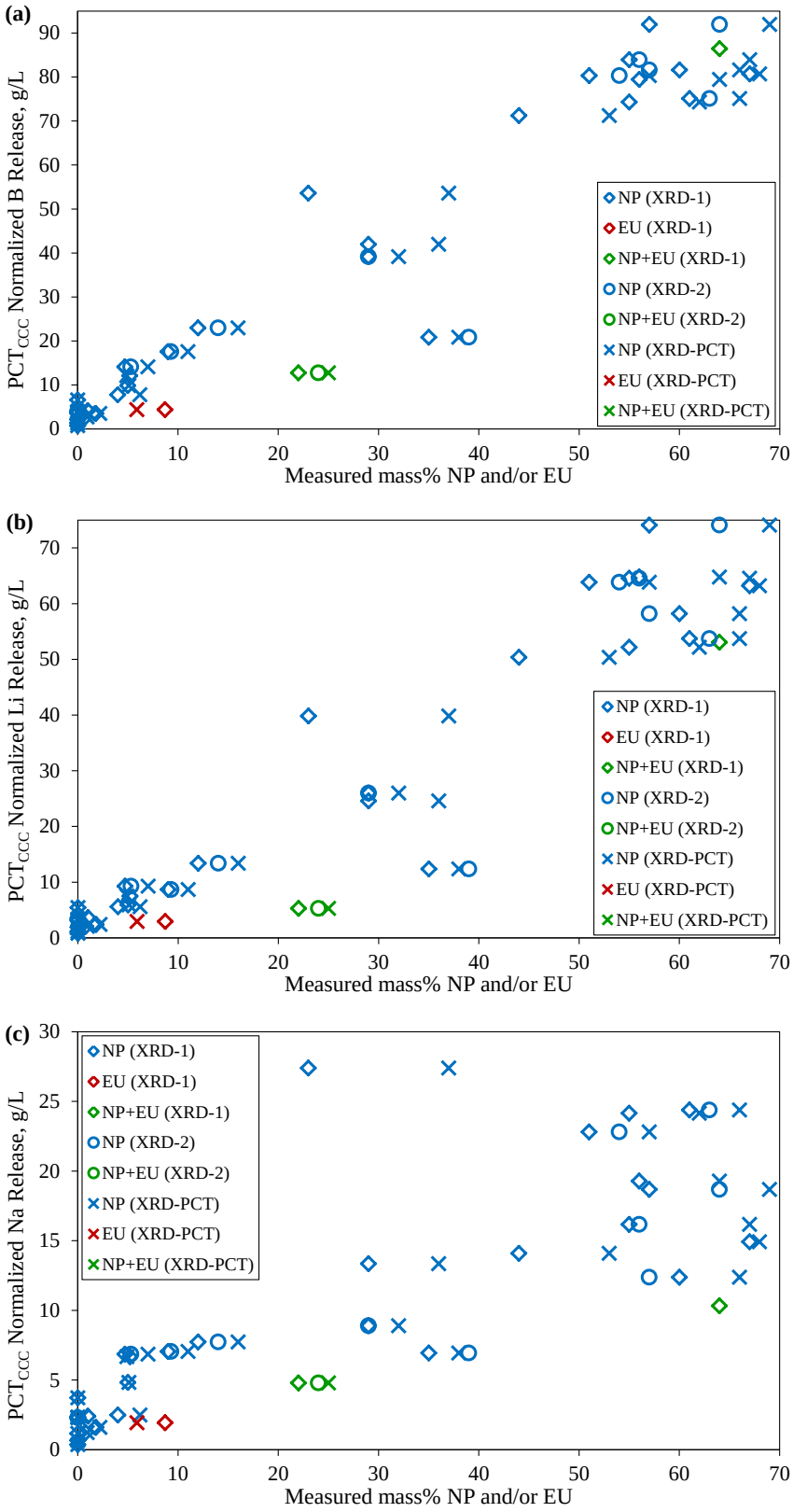

Figure 6.2. Measured mass% of Crystal vs Normalized PCT Release of (a) B, (b) Li, and (c) Na (NP = Nepheline, EU = Eucryptite)

To help visualize the effect of nepheline crystal fraction on PCT response, the natural logarithm of the NC_B of the quenched glasses were subtracted from the respective natural logarithm of NC_B of CCC glasses and plotted against the measured nepheline plus eucryptite concentration in Figure 6.3. In Figure 6.3, glasses that precipitated only nepheline (NP) are plotted in blue, the glass that precipitated only eucryptite (EU) is plotted in red, and the glasses that precipitated nepheline and eucryptite are plotted in green. The symbols represent the various samples analyzed, and can be related back to the sub-sample IDs in Table 5.1. Figure 6.3 has not been reviewed according to NQAP procedures and should be considered FIO.

In Figure 6.3, the difference between the natural logarithms of PCT B releases for the quenched and CCC glasses increases with increasing crystal concentration. This relationship indicates the detrimental effect of nepheline on glass durability. The two data points that appear to not follow the trend (circled in orange) are from glass "NP2-Very Low Si" and can be explained by the high NC_B of the quenched glass. The NC_B response of the quenched glass (15.4 g/L) is roughly the same as that of the EA glass (NC_B = 16.7 ±2.4) and roughly four times higher than other glasses in this study. Because the quenched glass values are subtracted from the CCC glass values in Figure 6.3, the formation of nepheline does not increase the NC_B as much.

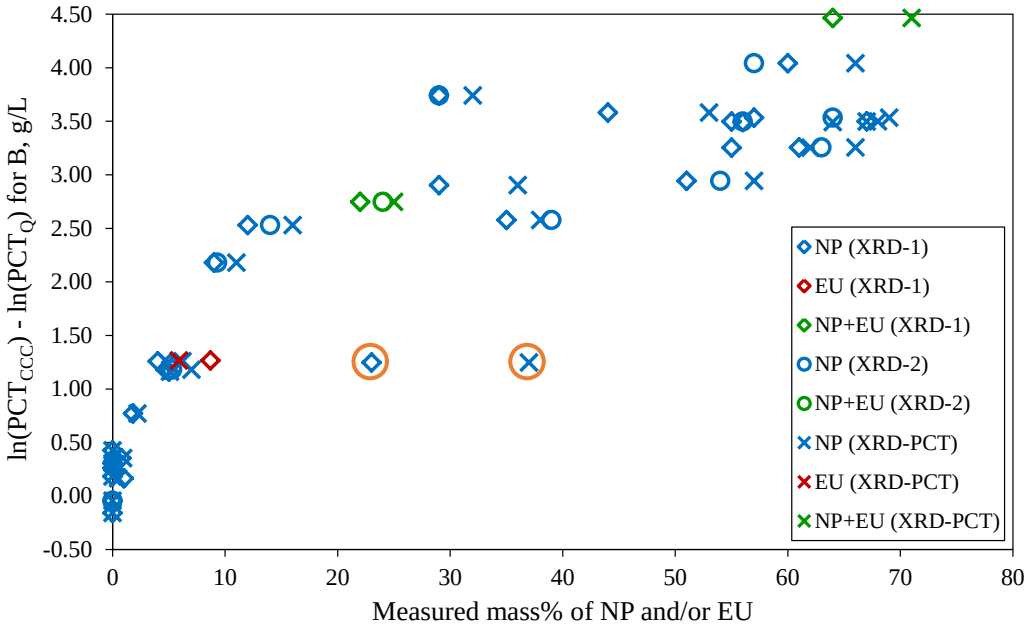

Figure 6.3. Natural Logarithm (ln) of Normalized B Release of Quenched Glasses Subtracted from the Natural Logarithm of Normalized B Release of CCC Glasses Plotted against Measured mass% of Nepheline (NP) and/or Eucryptite (EU). Orange circles indicate glass NP2-Very Low Si. (This Figure is For Information Only)

The purpose of the work presented in this report was to generate data for modeling the effects of HLW glass compositions on nepheline formation and nepheline fraction, and ultimately on the PCT response. Future modeling efforts should use the targeted glass compositions identified in Table 3.2, with the exception of glass NP2-High Na. Glass NP2-High Na was likely misbatched (see Section 5.2), and the composition was adjusted. In this case, the adjusted composition (denoted as NP2-High Na* in Table 3.2) should be used for modeling.

7.0 References

10 CFR 830, Subpart A. 2010. “Nuclear Safety Management.” Subpart A, “Quality Assurance Requirements.” *Code of Federal Regulations*, U.S. Department of Energy. Available at http://ecfr.gpoaccess.gov/cgi/t/text/textidx?c=ecfr&rgn=div6&view=text&node=10:4.0.2.5.26.1&idno=10.

ASME. 2001. *Quality Assurance Requirements for Nuclear Facility Applications*. ASME NQA-1-2000, American Society of Mechanical Engineers, New York, New York.

ASME. 2008. *Quality Assurance Requirements for Nuclear Facility Applications*. ASME NQA-1-2008, American Society of Mechanical Engineers, New York, New York.

ASME. 2009. *Addenda to NQA-1-2008, Quality Assurance Requirements for Nuclear Facility Applications*. ASME NQA-1a-2009, American Society of Mechanical Engineers, New York, New York.

ASME. 2013. *Quality Assurance Requirements for Nuclear Facility Applications*. ASME NQA-1-2012, American Society of Mechanical Engineers, New York, New York.

ASTM. 2014. *Standard Test Methods for Determining Chemical Durability of Nuclear Waste Glasses: The Product Consistency Test (PCT)*. ASTM C-1285, ASTM International. West Conshohocken, Pennsylvania.

Atkinson, AC, AN Donev, and RD Tobias. 2007. *Optimum Experimental Designs, with SAS.* Oxford Statistical Science Series, Oxford University Press, Oxford, United Kingdom.

Cheary, RW, AA Coelho, and JP Cline. 2004. “Fundamental Parameters Line Profile Fitting in Laboratory Diffractometers.” *Journal of Research of the National Institute of Standards and Technology* 109(1):1-25. Available at http://nvlpubs.nist.gov/nistpubs/jres/109/1/j91che.pdf.

Cornell, JA. 2002. *Experiments With Mixtures: Designs, Models, and the Analysis of Mixture Data, Third Edition.* John Wiley & Sons, New York. ISBN: 978-0-471-39367-2.

DOE Order 414.1D, *Quality Assurance*. U.S. Department of Energy, Washington, D.C.

U.S. Department of Energy, Office of River Protection (DOE-ORP). *Design, Construction, and Commissioning of the Hanford Tank Waste Treatment and Immobilization Plant.* Richland, Washington.

Fox, KM, TB Edwards, and D L McClane. 2016. *Chemical Composition Analysis and Product Consistency Tests Supporting Refinement of the Nepheline Model for the High Aluminum Hanford Glass Composition Region*. SRNL-STI-2016-00028, Rev. 1. Savannah River National Laboratory, Aiken, South Carolina.

Hrma, PR and GF Piepel. 1994. *Property/Composition Relationships for Hanford High-Level Waste Glasses Melting at 1150°C, Volume 2, Chapters 12-16 and Appendices A-K*. PNL-10359. Pacific Northwest National Laboratory, Richland, Washington.

Jantzen, CM, NE Bibler, DC Beam, CL Crawford, and MA Pickett. 1993. *Characterization of the Defense Waste Processing Facility (DWPF) Environmental Assessment (EA) Glass Standard Reference Material,* WSRC-TR-92-346, Revision 1. Westinghouse Savannah River Company, Aiken, South Carolina.

Kim, D-S, D Peeler, and P Hrma. 1995. "Effect of Crystallization on the Chemical Durability of Simulated Nuclear Waste Glasses." *Ceramic Transactions* 61:177-185.

Li, H, JD Vienna, P Hrma, DE Smith, and MJ Schweiger. 1997. "Nepheline Precipitation in High-Level Waste Glasses: Compositional Effects and Impact on the Waste Form Acceptability." *Scientific Basis for Nuclear Waste Management XX.* 465:261-268. Materials Research Society, Pittsburgh, Pennsylvania.

McCloy, J and JD Vienna. 2010. *Glass Composition Constraint Recommendations for Use in Life-Cycle Mission Modeling.* PNNL-19372. Pacific Northwest National Laboratory, Richland, Washington. Availale at http://www.pnl.gov/main/publications/external/technical_reports/PNNL-19372.pdf.

McCloy, JS, MJ Schweiger, CP Rodriguez, and JD Vienna. 2011. "Nepheline Crystallization in Nuclear Waste Glasses: Progress toward Acceptance of High-Alumina Formulations." *International Journal of Applied Glass Science* 2(3):201-214. Available at http://onlinelibrary.wiley.com/doi/10.1111/j.2041-1294.2011.00055.x/full.

Rodriguez, CP, JS McCloy, MJ Schweiger, JV Crum, and A Winschell. 2011. *Optical Basicity and Nepheline Crystallization in High Alumina Glasses.* PNNL-20184. Pacific Northwest National Laboratory, Richland, Washington. Available at http://www.pnnl.gov/main/publications/external/technical_reports/PNNL-20184.pdf.

Vienna, JD, A Fluegel, DS Kim, and P Hrma. 2009. *Glass Property Data and Models for Estimating High-Level Waste Glass Volume.* PNNL-18501, Pacific Northwest National Laboratory Richland, Washington. Available at http://www.pnl.gov/main/publications/external/technical_reports/PNNL-18501.pdf.

Vienna, JD, D-S Kim, DC Skorski, and J Matyas. 2013. *Glass Property Models and Constraints for Estimating the Glass to Be Produced at Hanford by Implementing Current Advanced Glass Formulation Efforts.* PNNL-22631, Rev. 1/ORP-58289, Pacific Northwest National Laboratory, Richland, Washington. Available at http://www.pnnl.gov/main/publications/external/technical_reports/PNNL-22631Rev1.pdf.

Vienna, JD, GF Piepel, DS Kim, JV Crum, CE Lonergan, BA Stanfill, BJ Riley, SK Cooley, and T Jin. 2016. *Update of Hanford Glass Property Models and Constraints for Use in Estimating the Glass Mass to be Produced at Hanford by Implementing Current Enhanced Glass Formulation Efforts.* PNNL-25835, Pacific Northwest National Laboratory, Richland, Washington. Available at http://www.pnnl.gov/main/publications/external/technical_reports/PNNL-25835.pdf.

Weier, DR and GF Piepel. 2003. *Methodology for Adjusting and Normalizing Analyzed Glass Composition*. PNWD-3260/WTP-RPT-049. Battelle Pacific Northwest Division, Richland, Washington. Available at http://www.pnl.gov/rpp-wtp/documents/WTP-RPT-049.pdf.

Welch, WJ. 1984. “Computer-Aided Design of Experiments for Response Estimation.” *Technometrics* 26:217-224.

Welch, WJ. 1987. *ACED, Algorithms for the Construction of Experimental Designs, Users Guide Version 1.6.1.* University of Waterloo,Waterloo, Ontario, Canada.

Appendix A

Quantitative XRD Results for Major Crystalline Phases

Appendix A

Quantitative XRD Results for Major Crystalline Phases

This appendix contains the quantitative XRD results for all crystalline phases ≥1 mass% in quenched and CCC glasses. In Table A.1, the Glass IDs, study phase, sub-sample IDs, and heat treatment (WTP-1 CCC, WTP-2 CCC, or quenched) are listed in their respective columns. In addition, this table contains the nepheline (NP) and eucryptite (EU) fractions and size of the crucible used for the CCC heat treatment. The crystalline phases identified in each sample (other than nepheline and eucryptite) are listed in the "Other Crystalline Species" column. The respective ICSD collection code for each crystalline phase identified is also listed in the table. The results associated with all Phase 1 glasses, except the single WWFTP QA qualified Phase 1 glass (Neph-NN-1-12), as well as baseline glasses BL1, BL2, and BL4 are considered FIO (see Section 2.2).

Table A.1. Quantitative XRD Results for all Major Crystalline Phases

Glass ID	Phase	Sub-Sample ID	Heat Treatment	CCC Crucible Size	NP[a] (Mass%)	CC[b]	EU[c] (Mass%)	CC[b]	Other Crystalline Species (CC[b]), Mass%
BL1[d]	-	BL1-CCC-XRD-1	WTP-1	1.2cm^3	45[d]		0[d]		Trevorite, 3.4[d]
BL2[d]	-	BL2-CCC-XRD-1	WTP-1	1.2cm^3	41[d]		0[d]		Trevorite, 3.6[d]
BL4[d]	-	BL4-CCC-XRD-1	WTP-1	1.2cm^3	26[d]		0[d]		Trevorite, 3.5[d]
Neph-NN-1-01[d][e]	1	Neph-NN-1-01-CCC-XRD-1	WTP-1	1.2cm^3	0[d]		0[d]		Lithium Iron Manganese Oxide (51693), 3.9[d]
Neph-NN-1-02[d]	1	Neph-NN-1-02-CCC-XRD-1	WTP-1	1.2cm^3	0[d]		0[d]		Lithium Iron Manganese Oxide (51693), 3.4[d]
Neph-NN-1-03[d]	1	Neph-NN-1-03-CCC-XRD-1	WTP-1	1.2cm^3	0[d]		0[d]		Nichromite, 3.4[d]
		Neph-NN-1-03-CCC-XRD-2	WTP-1	1.2cm^3	0[d]		0[d]		Nichromite, 3.1[d]
Neph-NN-1-04[d]	1	Neph-NN-1-04-CCC-XRD-1	WTP-1	1.2cm^3	0[d]		0[d]		Nichromite, 8.4[d]
Neph-NN-1-05[d]	1	Neph-NN-1-05-CCC-XRD-1	WTP-1	1.2cm^3	0[d]		0[d]		Nichromite, 4.1[d]
		Neph-NN-1-05-CCC-XRD-2	WTP-1	1.2cm^3	0[d]		0[d]		Nichromite, 3.7[d]
Neph-NN-1-06[d]	1	Neph-NN-1-06-CCC-XRD-1	WTP-1	1.2cm^3	0[d]		0[d]		Nichromite, 1.8[d]
		Neph-NN-1-06-CCC-XRD-2	WTP-1	1.2cm^3	0[d]		0[d]		Nichromite, 1.7[d]
Neph-NN-1-07[d]	1	Neph-NN-1-07-CCC-XRD-1	WTP-1	1.2cm^3	0[d]		0[d]		Trevorite, 2.4[d]
		Neph-NN-1-07-CCC-XRD-2	WTP-1	1.2cm^3	0[d]		0[d]		Trevorite, 2.2[d]
Neph-NN-1-08[d]	1	Neph-NN-1-08-CCC-XRD-1	WTP-1	1.2cm^3	0[d]		0[d]		Lithium Iron Oxide, 2.7[d]
Neph-NN-1-09[d]	1	Neph-NN-1-09-CCC-XRD-1	WTP-1	1.2cm^3	0[d]		0[d]		Nichromite, 5.3[d]
Neph-NN-1-10[d]	1	Neph-NN-1-10-CCC-XRD-1	WTP-1	1.2cm^3	0[d]		0[d]		Nichromite, 4.7[d]
Neph-NN-1-11[d]	1	Neph-NN-1-11-CCC-XRD-1	WTP-1	1.2cm^3	0[d]		0[d]		Nichromite, 3.1[d]
Neph-NN-1-12	1	Neph-NN-1-12-CCC-XRD-1	WTP-1	1.2cm^3	55	155002	0		Lithium Iron Oxide, 2.8
		Neph-NN-1-12-CCC-XRD-2	WTP-1	1.2cm^3	56	155002	0		Lithium Iron Oxide, 2.2
		Neph-NN-1-12-CCC-PCT	WTP-2	1in^3	67	155002	0		Trevorite (52387), 3.2 Lithium Aluminum Oxide (23815), 1.1
		Neph-NN-1-12-Q-PCT	Q		0		0		None
Neph-NN-1-13[d]	1	Neph-NN-1-13-CCC-XRD-1	WTP-1	1.2cm^3	0[d]		0[d]		Lithium Iron Manganese Oxide, 6.2[d]
Neph-NN-1-14[d]	1	Neph-NN-1-14-CCC-XRD-1	WTP-1	1.2cm^3	0[d]		0[d]		Lithium Iron Manganese Oxide, 5.5[d]
Neph-NN-1-15[d]	1	Neph-NN-1-15-CCC-XRD-1	WTP-1	1.2cm^3	0[d]		0[d]		Lithium Iron Oxide, 1.7[d] Lithium Iron Chromium Oxide (21092), 2.0[d]

Table A.1. Quantitative XRD Results for all Major Crystalline Phases (cont'd)

Glass ID	Phase	Sub-Sample ID	Heat Treatment	CCC Crucible Size	NP[(a)] (Mass%)	CC[(b)]	EU[(c)] (Mass%)	CC[(b)]	Other Crystalline Species (CC[(b)]), Mass%
BL3	2	BL3-CCC-XRD-1	WTP-2	1.2cm^3	12	155002	0		Lithium Iron Oxide (155029), 1.7 Lithium Iron Manganese Oxide (93817), 2.0
		BL3-CCC-XRD-2	WTP-2	1.2cm^3	14	155002	0		Lithium Iron Oxide (51206), 2.3 Lithium Iron Manganese Oxide (93817), 1.6
		BL3-CCC-PCT	WTP-2	1in^3	16	155002	0		Lithium Iron Oxide (155029), 2.1 Lithium Iron Manganese Oxide (93817), 2.2
		BL3-Q-PCT	Q		0		0		Lithium Iron Manganese Oxide (150249), 2.8
NP2-High Al	2	NP2-HighAl-CCC-XRD-1	WTP-2	1.2cm^3	9.0	155002	0		Lithium Iron Manganese Oxide (88142), 2.3 Lithium Iron Chromium Oxide (21091), 2.5
		NP2-HighAl-CCC-XRD-2	WTP-2	1.2cm^3	9.3	155002	0		Lithium Iron Manganese Oxide (88142), 2.4 Lithium Iron Chromium Oxide (21091), 2.3
		NP2-HighAl-CCC-PCT	WTP-2	1in^3	11	155002	0		Lithium Iron Manganese Oxide (88142), 6.4
NP2-High B	2	NP2-HighB-CCC-XRD-1	WTP-2	1.2cm^3	1.0	155001	0		Lithium Iron Oxide (51206), 2.9
		NP2-HighB-CCC-PCT	WTP-2	1in^3	0.48	155001	0		Lithium Iron Oxide (51206), 3.6
NP2-High Li	2	NP2-HighLi-CCC-XRD-1	WTP-2	1.2cm^3	44	155002	0		Lithium Iron Manganese Oxide (93817), 2.1 Iron Oxide (87121), 1.6
		NP2-HighLi-CCC-PCT	WTP-2	1in^3	53	155002	0		Lithium Iron Manganese Oxide (93817), 2.5 Iron Oxide (87121), 1.9
NP2-High Na	2	NP2-HighNa-CCC-XRD-1	WTP-2	1.2cm^3	56	155002	0		Iron Oxide (87121), 3.1
		NP2-HighNa-CCC-PCT	WTP-2	1in^3	64	155002	0		Lithium Iron Oxide (51206), 1.8 Lithium Iron Manganese Oxide (93817), 2.3
NP2-High Si	2	NP2-HighSi-CCC-XRD-1	WTP-2	1.2cm^3	29	155002	0		Lithium Iron Oxide (51206), 1.7 Lithium Iron Manganese Oxide (93817), 1.4
		NP2-HighSi-CCC-XRD-2	WTP-2	1.2cm^3	29	155002	0		Lithium Iron Oxide (51206), 2.0 Lithium Iron Manganese Oxide (93817), 1.1
		NP2-HighSi-CCC-PCT	WTP-2	1in^3	32	155002	0		Lithium Iron Oxide (51206), 3.2 Lithium Iron Manganese Oxide (93817), 1.3
NP2-Low Al	2	NP2-LowAl-CCC-XRD-1	WTP-2	1.2cm^3	4.0	155002	0		Lithium Iron Manganese Oxide (93817), 3.1
		NP2-LowAl-CCC-PCT	WTP-2	1in^3	6.2	155002	0		Lithium Iron Manganese Oxide (93817), 3.5

Table A.1. Quantitative XRD Results for all Major Crystalline Phases (cont'd)

Glass ID	Phase	Sub-Sample ID	Heat Treatment	CCC Crucible Size	NP[(a)] (Mass%)	CC[(b)]	EU[(c)] (Mass%)	CC[(b)]	Other Crystalline Species (CC[(b)]), Mass%
NP2-Low B	2	NP2-LowB-CCC-XRD-1	WTP-2	1.2cm^3	60	155002	0		Iron Oxide (70048, 87121), 3.2 Lithium Iron Manganese Oxide (93823), 1.0
		NP2-LowB-CCC-XRD-2	WTP-2	1.2cm^3	57	155002	0		Iron Oxide (70048, 87121), 3.0 Lithium Iron Manganese Oxide (93823), 1.1
		NP2-LowB-CCC-PCT	WTP-2	1in^3	66	155002	0		Lithium Iron Oxide (51206), 4.0
NP2-Low Li	2	NP2-LowLi-CCC-XRD-1	WTP-2	1.2cm^3	1.8	155002	0		Lithium Iron Oxide (51206), 2.6 Lithium Iron Manganese Oxide (93817), 1.1
		NP2-LowLi-CCC-PCT	WTP-2	1in^3	2.2	155002	0		Lithium Iron Oxide (51206), 2.9 Lithium Iron Manganese Oxide (93817), 1.2
NP2-Low Na	2	NP2-LowNa-CCC-XRD-1	WTP-2	1.2cm^3	0		8.7	66137	Lithium Iron Manganese Oxide (150251), 3.9
		NP2-LowNa-CCC-PCT	WTP-2	1in^3	0		5.9	66137	Lithium Iron Manganese Oxide (150251), 5.3
		NP2-LowNa-Q-PCT	Q		0		0		Iron Silicon Oxide (41006), 2.1 Eskolaite (250078), 1.4
NP2-Low Si	2	NP2-LowSi-CCC-XRD-1	WTP-2	1.2cm^3	5.0	155002	0		Lithium Iron Manganese Oxide (150251, 155280), 3.6
		NP2-LowSi-CCC-PCT	WTP-2	1in^3	5.1	155002	0		Lithium Iron Manganese Oxide (93827), 1.2 Iron Oxide (70048), 3.4
NP2-Very High Al	2	NP2-VeryHighAl-CCC-XRD-1	WTP-2	1.2cm^3	29	155002	0		Aluminum Oxide (69213), 13
		NP2-VeryHighAl-CCC-PCT	WTP-2	1in^3	36	155002	0		Aluminum Oxide (69213), 16 Iron Oxide (70048), 1.1
NP2-Very High Si	2	NP2-VeryHighSi-CCC-XRD-1	WTP-2	1.2cm^3	0		0		Chromite (171121), 2.0
		NP2-VeryHighSi-CCC-PCT	WTP-2	1in^3	0		0		Chromite (171121), 2.3
NP2-Very Low Si	2	NP2-VeryLowSi-CCC-XRD-1	WTP-2	1.2cm^3	23	155002	0		Lithium Iron Manganese Oxide (150249), 1.5 Lithium Iron Chromium Oxide (21090), 4.0
		NP2-VeryLowSi-CCC-PCT	WTP-2	1in^3	37	155002	0		Lithium Iron Manganese Oxide (88142), 8.0
		NP2-VeryLowSi-Q-PCT	Q		0		0		Lithium Iron Chromium Oxide (21092), 4.0
NP-MC-AlB-1	3	NP-MC-AlB-1-CCC-XRD-1	WTP-2	1.2cm^3	0		0		Lithium Iron Manganese Oxide (93817), 3.2
		NP-MC-AlB-1-CCC-XRD-2	WTP-2	1.2cm^3	0		0		Lithium Iron Manganese Oxide (93817), 3.3
		NP-MC-AlB-1-CCC-PCT	WTP-2	1in^3	0		0		Lithium Iron Manganese Oxide (93817), 3.3

Table A.1. Quantitative XRD Results for all Major Crystalline Phases (cont'd)

Glass ID	Phase	Sub-Sample ID	Heat Treatment	CCC Crucible Size	NP[(a)] (Mass%)	CC[(b)]	EU[(c)] (Mass%)	CC[(b)]	Other Crystalline Species (CC[(b)]), Mass%
NP-MC-AlBNa-1	3	NP-MC-AlBNa-1-CCC-XRD-1	WTP-2	1.2cm^3	0		0		Lithium Iron Oxide (51206), 2.1 Lithium Iron Manganese Oxide (93817), 1.6
		NP-MC-AlBNa-1-CCC-PCT	WTP-2	1in^3	0		0		Lithium Iron Oxide (51206), 2.0 Lithium Iron Manganese Oxide (93817), 1.9
NP-MC-AlBNa-2	3	NP-MC-AlBNa-2-CCC-XRD-1	WTP-2	1.2cm^3	5.2	155002	0		Iron Oxide (70048), 2.5 Lithium Iron Manganese Oxide (93827), 1.1
		NP-MC-AlBNa-2-CCC-PCT	WTP-2	1in^3	4.9	155002	0		Lithium Iron Manganese Oxide (93817), 2.5 Iron Oxide (70048), 1.1
NP-MC-AlBSi-1	3	NP-MC-AlBSi-1-CCC-XRD-1	WTP-2	1.2cm^3	0		0		Iron Chromium Oxide (163943), 1.4 Sodium Aluminum Oxide (32600), 1.9
		NP-MC-AlBSi-1-CCC-PCT	WTP-2	1in^3	0		0		Iron Chromium Oxide (163943), 1.2 Sodium Aluminum Oxide (32600), 1.7
		NP-MC-AlBSi-1-Q-PCT	Q		0		0		None
NP-MC-AlLi-1	3	NP-MC-AlLi-1-CCC-XRD-1	WTP-2	1.2cm^3	0.77	155001	0		Iron Silicon Oxide (87459), 3.2
		NP-MC-AlLi-1-CCC-PCT	WTP-2	1in^3	0.94	155001	0		Iron Oxide (77588), 2.8
NP-MC-AlLi-2	3	NP-MC-AlLi-2-CCC-XRD-1	WTP-2	1.2cm^3	35	155002	0		Lithium Iron Oxide (51665), 1.7
		NP-MC-AlLi-2-CCC-XRD-2	WTP-2	1.2cm^3	39	155002	0		Lithium Iron Oxide (51665), 3.3
		NP-MC-AlLi-2-CCC-PCT	WTP-2	1in^3	38	155002	0		Lithium Iron Manganese Oxide (150251), 4.5
		NP-MC-AlLi-2-Q-PCT	Q		0		0		Iron Silicon Oxide (87460), 2.7
NP-MC-AlLiNa-1	3	NP-MC-AlLiNa-1-CCC-XRD-1	WTP-2	1.2cm^3	61	155001, 85553	0		Lithium Iron Manganese Oxide (88142), 5.0 Lithium Aluminum Borate (51754), 9.6
		NP-MC-AlLiNa-1-CCC-XRD-2	WTP-2	1.2cm^3	63	155001, 85553	0		Lithium Iron Manganese Oxide (150249, 150239, 88142), 5.2 Lithium Aluminum Borate (51754), 12
		NP-MC-AlLiNa-1-CCC-PCT	WTP-2	1in^3	66	155001, 85553	0		Lithium Iron Manganese Oxide (150249, 150239), 5.1 Lithium Aluminum Borate (51754), 11

Table A.1. Quantitative XRD Results for all Major Crystalline Phases (cont'd)

Glass ID	Phase	Sub-Sample ID	Heat Treatment	CCC Crucible Size	NP[(a)] (Mass%)	CC[(b)]	EU[(c)] (Mass%)	CC[(b)]	Other Crystalline Species (CC[(b)]), Mass%
NP-MC-AlLiSi-1	3	NP-MC-AlLiSi-1-CCC-XRD-1	WTP-2	1.2cm^3	4.7	155002	0		Lithium Iron Manganese Oxide (93817), 1.2 Iron Silicon Oxide (87459), 2.5
		NP-MC-AlLiSi-1-CCC-XRD-2	WTP-2	1.2cm^3	5.3	155002	0		Lithium Iron Manganese Oxide (93817), 1.7 Iron Silicon Oxide (87459), 2.5
		NP-MC-AlLiSi-1-CCC-PCT	WTP-2	1in^3	7.0	155002	0		Lithium Iron Manganese Oxide (93817), 1.8 Iron Silicon Oxide (87459), 2.6
NP-MC-AlNa-1	3	NP-MC-AlNa-1-CCC-XRD-1	WTP-2	1.2cm^3	57	155002	0		Lithium Iron Manganese Oxide (155280), 1.1 Iron Oxide (79196), 2.1 Nosean (18125), 1.3
		NP-MC-AlNa-1-CCC-XRD-2	WTP-2	1.2cm^3	64	155002	0		Lithium Iron Manganese Oxide (155280, 93817), 2.9 Iron Oxide (79196), 1.2 Nosean (18125), 1.6
		NP-MC-AlNa-1-CCC-PCT	WTP-2	1in^3	69	155002	0		Lithium Iron Manganese Oxide (93817), 3.4 Iron Oxide (79196), 1.1
NP-MC-AlSi-1	3	NP-MC-AlSi-1-CCC-XRD-1	WTP-2	1.2cm^3	51	155002	0		Lithium Iron Oxide (155029), 3.3 Lithium Iron Manganese Oxide (93823), 1.6
		NP-MC-AlSi-1-CCC-XRD-2	WTP-2	1.2cm^3	54	155002	0		Lithium Iron Oxide (155029), 3.4 Lithium Iron Manganese Oxide (93823), 1.5
		NP-MC-AlSi-1-CCC-PCT	WTP-2	1in^3	57	155002	0		Lithium Iron Oxide (155029), 3.3 Lithium Iron Manganese Oxide (93823), 1.5
NP-MC-AlSi-2	3	NP-MC-AlSi-2-CCC-XRD-1	WTP-2	1.2cm^3	8.9	155002	13	66137	Iron Chromium Oxide (163943), 1.3 Eskolaite (201105), 1.1 Aluminum Chromium Oxide (9545), 1.2
		NP-MC-AlSi-2-CCC-XRD-2	WTP-2	1.2cm^3	9.5	155002	14	66137	Iron Chromium Oxide (163943), 1.3 Eskolaite (201105), 1.2
		NP-MC-AlSi-2-CCC-PCT	WTP-2	1in^3	11	155002	14	66137	Iron Chromium Oxide (163943), 1.4 Eskolaite (201105), 1.4 Aluminum Chromium Oxide (9545), 1.7

Table A.1. Quantitative XRD Results for all Major Crystalline Phases (cont'd)

Glass ID	Phase	Sub-Sample ID	Heat Treatment	CCC Crucible Size	NP[(a)] (Mass%)	CC[(b)]	EU[(c)] (Mass%)	CC[(b)]	Other Crystalline Species (CC[(b)]), Mass%
NP-MC-BLiSi-1	3	NP-MC-BLiSi-1-CCC-XRD-1	WTP-2	1.2cm^3	59	155002, 155001	5.2	66137	Lithium Iron Manganese Oxide (93817), 2.9 Iron Oxide (87121), 1.2 Silicon Oxide (170483), 1.1
		NP-MC-BLiSi-1-CCC-PCT	WTP-2	1in^3	63	155002	7.9	66137, 32595	Lithium Iron Oxide (51206), 1.7 Lithium Iron Manganese Oxide (93817), 2.1
		NP-MC-BLiSi-1-Q-PCT	Q		0		0		Lithium Iron Manganese Oxide (150251, 150247), 2.7
NP-MC-BLiSi-2	3	NP-MC-BLiSi-2-CCC-XRD-1	WTP-2	1.2cm^3	0		0		Lithium Iron Manganese Oxide (93817), 2.1 Iron Oxide (79196), 1.2
		NP-MC-BLiSi-2-CCC-PCT	WTP-2	1in^3	0		0		Lithium Iron Manganese Oxide (93817), 2.3 Iron Oxide (79196), 1.0
NP-MC-BNa-1	3	NP-MC-BNa-1-CCC-XRD-1	WTP-2	1.2cm^3	67	155002, 155001	0		Lithium Iron Oxide (155029), 2.9 Lithium Iron Manganese Oxide (93823), 1.3
		NP-MC-BNa-1-CCC-PCT	WTP-2	1in^3	68	155002	0		Lithium Iron Oxide (155029), 2.8 Lithium Iron Manganese Oxide (93823), 1.7
		NP-MC-BNa-1-Q-PCT	Q		3.1	155002	0		Lithium Iron Manganese Oxide (150247), 1.8 Iron Oxide (35643), 1.1
NP-MC-BNaSi-1	3	NP-MC-BNaSi-1-CCC-XRD-1	WTP-2	1.2cm^3	55	155002, 155001	0		Lithium Iron Manganese Oxide (150249, 150239), 7.2
		NP-MC-BNaSi-1-CCC-PCT	WTP-2	1in^3	62	155002, 155001	0		Lithium Iron Manganese Oxide (150249), 1.6 Iron Oxide (87121), 4.1
NP-MC-BSi-1	3	NP-MC-BSi-1-CCC-XRD-1	WTP-2	1.2cm^3	0		0		Eskolaite (250078), 1.2
		NP-MC-BSi-1-CCC-PCT	WTP-2	1in^3	0		0		Iron Oxide (35002), 1.4

(a) NP = Nepheline
(b) CC = Inorganic Crystal Structure Database Collection Code
(c) EU = Eucryptite
(d) Data are considered FIO
(e) Neph-NN-1-01 is BL0

Appendix B

XRD Spectrum for the Glass with Unfit Peaks

Appendix B

XRD Spectrum for the Glass with Unfit Peaks

This appendix contains the XRD spectrum of the CCC version of glass NP-MC-AlBSi-1, for which an appropriate pattern could not be identified for fitting. The unfit peaks are identified by black arrows in Figure B.1. It should be noted that all peaks associated with nepheline were successfully identified and fit.

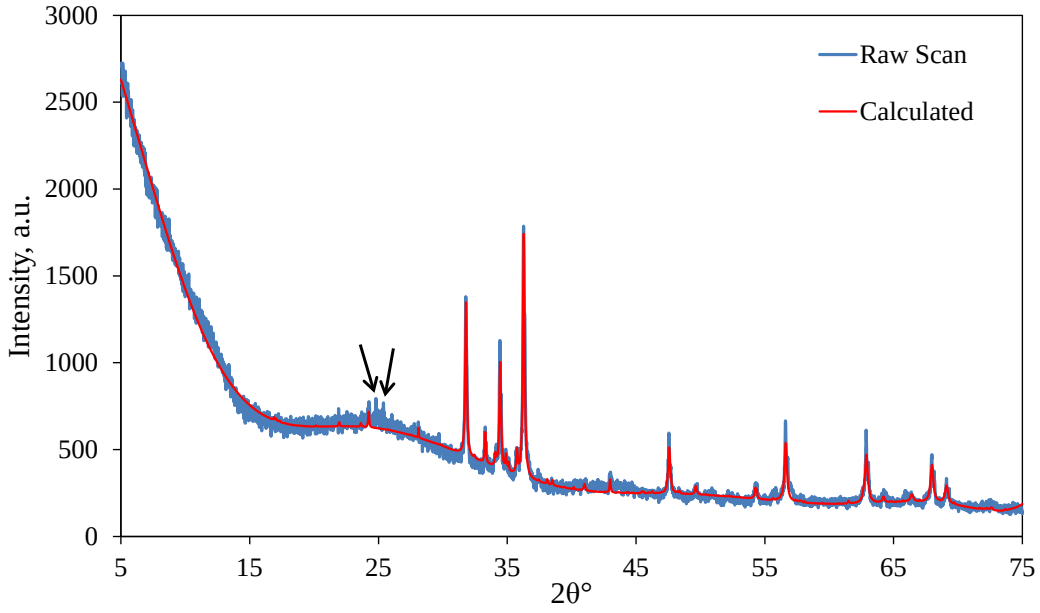

Figure B.1. XRD Pattern from NP-MC-AlBSi-1 CCC Sample (Blue line = raw scan, red line = calculated pattern, black arrows identify unfit peaks)

Appendix C

Composition Analysis Results

Appendix C

Composition Analysis Results

This appendix contains the composition analysis results reported by Fox et al. (2016). The components F and RuO_2 were not included in the composition analyses, as discussed in Section 4.4. The "Measured" values in Table C.1 are the average of two measurements taken from each prepared sample. All measured oxides with concentrations below the associated detection limit are denoted by a less than symbol (<) in the below detectable limits column. The difference and percent relative difference between measured and targeted values was not computed for oxides with concentrations below detectable limits. The average measured oxide concentrations in the low-activity reference material (LRM) are also reported. For the LRM glass, the "Targeted" oxide concentrations represent the nominal oxide concentrations.

Table C.1. Composition Analysis Results Including Reference Material

Glass ID[(a)]	Oxide	BDL (<)[(b)]	Measured (mass%)	Targeted (mass%)	Difference of Measured Versus Targeted (mass%)	%Relative Difference of Measured versus Targeted
LRM	Al_2O_3		9.50	9.51	-0.01	-0.1%
LRM	B_2O_3		7.66	7.85	-0.19	-2.4%
LRM	Bi_2O_3	<	0.11	0.00		
LRM	CaO		0.46	0.54	-0.08	-14.8%
LRM	Cr_2O_3	<	0.16	0.19		
LRM	Fe_2O_3		1.43	1.38	0.05	3.6%
LRM	Li_2O	<	0.22	0.11		
LRM	MnO	<	0.13	0.08		
LRM	Na_2O		21.37	20.03	1.34	6.7%
LRM	NiO		0.18	0.19	-0.01	-5.3%
LRM	P_2O_5		0.49	0.54	-0.05	-9.3%
LRM	SiO_2		53.86	54.20	-0.34	-0.6%
LRM	SO_3		0.22	0.30	-0.08	-26.7%
LRM	ZrO_2		0.96	0.93	0.03	3.2%
LRM	Sum		96.75	95.85	0.90	0.9%
Neph-NN-1-12	Al_2O_3		26.45	26.92	-0.47	-1.7%
Neph-NN-1-12	B_2O_3		17.05	17.00	0.05	0.3%
Neph-NN-1-12	Bi_2O_3		0.64	0.71	-0.07	-9.9%
Neph-NN-1-12	CaO		0.43	0.47	-0.04	-8.5%
Neph-NN-1-12	Cr_2O_3		0.41	0.47	-0.06	-12.8%
Neph-NN-1-12	Fe_2O_3		2.33	2.36	-0.03	-1.3%
Neph-NN-1-12	Li_2O		5.51	5.67	-0.16	-2.8%
Neph-NN-1-12	MnO		0.88	0.94	-0.06	-6.4%

Table C.1. Composition Analysis Results Including Reference Material (cont'd)

Glass ID[a]	Oxide	BDL (<)[b]	Measured (mass%)	Targeted (mass%)	Difference of Measured Versus Targeted (mass%)	%Relative Difference of Measured versus Targeted
Neph-NN-1-12	Na_2O		16.07	15.00	1.07	7.1%
Neph-NN-1-12	NiO		0.19	0.24	-0.05	-20.8%
Neph-NN-1-12	P_2O_5		0.88	0.94	-0.06	-6.4%
Neph-NN-1-12	SiO_2		29.20	28.99	0.21	0.7%
Neph-NN-1-12	SO_3		0.25	0.24	0.01	4.2%
Neph-NN-1-12	Sum		100.29	99.95	0.34	0.3%
BL3	Al_2O_3		27.87	28.50	-0.63	-2.2%
BL3	B_2O_3		16.67	17.20	-0.53	-3.1%
BL3	Bi_2O_3		0.60	0.65	-0.05	-7.7%
BL3	CaO		0.60	0.65	-0.05	-7.7%
BL3	Cr_2O_3		0.99	1.10	-0.11	-10.0%
BL3	Fe_2O_3		2.52	2.50	0.02	0.8%
BL3	Li_2O		4.81	5.00	-0.19	-3.8%
BL3	MnO		0.91	1.00	-0.09	-9.0%
BL3	Na_2O		13.20	12.50	0.70	5.6%
BL3	P_2O_5		0.67	0.70	-0.03	-4.3%
BL3	SiO_2		29.52	29.35	0.17	0.6%
BL3	SO_3		0.26	0.25	0.01	4.0%
BL3	ZrO_2		0.25	0.25	0.00	0.0%
BL3	Sum		98.87	99.65	-0.78	-0.8%
NP2-High Al	Al_2O_3		31.22	31.50	-0.28	-0.9%
NP2-High Al	B_2O_3		16.48	16.48	0.00	0.0%
NP2-High Al	Bi_2O_3		0.57	0.62	-0.05	-8.1%
NP2-High Al	CaO		0.51	0.62	-0.11	-17.7%
NP2-High Al	Cr_2O_3		0.96	1.05	-0.09	-8.6%
NP2-High Al	Fe_2O_3		2.39	2.40	-0.01	-0.4%
NP2-High Al	Li_2O		4.60	4.79	-0.19	-4.0%
NP2-High Al	MnO		0.88	0.96	-0.08	-8.3%
NP2-High Al	Na_2O		12.75	11.98	0.77	6.4%
NP2-High Al	P_2O_5		0.63	0.67	-0.04	-6.0%
NP2-High Al	SiO_2		28.51	28.12	0.39	1.4%
NP2-High Al	SO_3		0.22	0.24	-0.02	-8.3%
NP2-High Al	ZrO_2		0.23	0.24	-0.01	-4.2%
NP2-High Al	Sum		99.95	99.67	0.28	0.3%
NP2-High B	Al_2O_3		26.50	26.85	-0.35	-1.3%
NP2-High B	B_2O_3		21.28	22.00	-0.72	-3.3%
NP2-High B	Bi_2O_3		0.57	0.61	-0.04	-6.6%
NP2-High B	CaO		0.50	0.61	-0.11	-18.0%

Table C.1. Composition Analysis Results Including Reference Material (cont'd)

Glass ID[a]	Oxide	BDL (<)[b]	Measured (mass%)	Targeted (mass%)	Difference of Measured Versus Targeted (mass%)	%Relative Difference of Measured versus Targeted
NP2-High B	Cr_2O_3		0.99	1.04	-0.05	-4.8%
NP2-High B	Fe_2O_3		2.45	2.36	0.09	3.8%
NP2-High B	Li_2O		4.71	4.71	0.00	0.0%
NP2-High B	MnO		0.96	0.94	0.02	2.1%
NP2-High B	Na_2O		12.33	11.78	0.55	4.7%
NP2-High B	P_2O_5		0.63	0.66	-0.03	-4.5%
NP2-High B	SiO_2		27.97	27.65	0.32	1.2%
NP2-High B	SO_3		0.19	0.24	-0.05	-20.8%
NP2-High B	ZrO_2		0.24	0.24	0.00	0.0%
NP2-High B	Sum		99.32	99.69	-0.37	-0.4%
NP2-High Li	Al_2O_3		28.06	28.20	-0.14	-0.5%
NP2-High Li	B_2O_3		17.22	17.02	0.20	1.2%
NP2-High Li	Bi_2O_3		0.59	0.64	-0.05	-7.8%
NP2-High Li	CaO		0.60	0.64	-0.04	-6.3%
NP2-High Li	Cr_2O_3		1.05	1.09	-0.04	-3.7%
NP2-High Li	Fe_2O_3		2.44	2.47	-0.03	-1.2%
NP2-High Li	Li_2O		5.76	6.00	-0.24	-4.0%
NP2-High Li	MnO		0.96	0.99	-0.03	-3.0%
NP2-High Li	Na_2O		13.25	12.37	0.88	7.1%
NP2-High Li	P_2O_5		0.66	0.69	-0.03	-4.3%
NP2-High Li	SiO_2		29.47	29.04	0.43	1.5%
NP2-High Li	SO_3		0.27	0.25	0.02	8.0%
NP2-High Li	ZrO_2		0.25	0.25	0.00	0.0%
NP2-High Li	Sum		100.58	99.65	0.93	0.9%
NP2-High Na	Al_2O_3		27.16	27.52	-0.36	-1.3%
NP2-High Na	B_2O_3		16.57	16.61	-0.04	-0.2%
NP2-High Na	Bi_2O_3		0.58	0.63	-0.05	-7.9%
NP2-High Na	CaO		0.59	0.63	-0.04	-6.3%
NP2-High Na	Cr_2O_3		0.96	1.06	-0.10	-9.4%
NP2-High Na	Fe_2O_3		2.37	2.41	-0.04	-1.7%
NP2-High Na	Li_2O		4.61	4.83	-0.22	-4.6%
NP2-High Na	MnO		0.89	0.97	-0.08	-8.2%
NP2-High Na	Na_2O		16.45	15.50	0.95	6.1%
NP2-High Na	P_2O_5		0.63	0.68	-0.05	-7.4%
NP2-High Na	SiO_2		28.56	28.34	0.22	0.8%
NP2-High Na	SO_3		0.26	0.24	0.02	8.3%
NP2-High Na	ZrO_2		0.46	0.24	0.22	91.7%
NP2-High Na	Sum		100.09	99.66	0.43	0.4%

Table C.1. Composition Analysis Results Including Reference Material (cont'd)

Glass ID[a]	Oxide	BDL (<)[b]	Measured (mass%)	Targeted (mass%)	Difference of Measured Versus Targeted (mass%)	%Relative Difference of Measured versus Targeted
NP2-High Si	Al_2O_3		26.78	27.03	-0.25	-0.9%
NP2-High Si	B_2O_3		16.04	16.31	-0.27	-1.7%
NP2-High Si	Bi_2O_3		0.57	0.62	-0.05	-8.1%
NP2-High Si	CaO		0.51	0.62	-0.11	-17.7%
NP2-High Si	Cr_2O_3		1.02	1.04	-0.02	-1.9%
NP2-High Si	Fe_2O_3		2.40	2.37	0.03	1.3%
NP2-High Si	Li_2O		4.60	4.74	-0.14	-3.0%
NP2-High Si	MnO		0.94	0.95	-0.01	-1.1%
NP2-High Si	Na_2O		12.57	11.85	0.72	6.1%
NP2-High Si	P_2O_5		0.62	0.66	-0.04	-6.1%
NP2-High Si	SiO_2		33.53	33.00	0.53	1.6%
NP2-High Si	SO_3		0.19	0.24	-0.05	-20.8%
NP2-High Si	ZrO_2		0.23	0.24	-0.01	-4.2%
NP2-High Si	Sum		100.00	99.67	0.33	0.3%
NP2-Low Al	Al_2O_3		24.99	25.50	-0.51	-2.0%
NP2-Low Al	B_2O_3		17.69	17.92	-0.23	-1.3%
NP2-Low Al	Bi_2O_3		0.62	0.68	-0.06	-8.8%
NP2-Low Al	CaO		0.58	0.68	-0.10	-14.7%
NP2-Low Al	Cr_2O_3		1.10	1.15	-0.05	-4.3%
NP2-Low Al	Fe_2O_3		2.56	2.60	-0.04	-1.5%
NP2-Low Al	Li_2O		4.96	5.21	-0.25	-4.8%
NP2-Low Al	MnO		0.99	1.04	-0.05	-4.8%
NP2-Low Al	Na_2O		13.35	13.02	0.33	2.5%
NP2-Low Al	P_2O_5		0.69	0.73	-0.04	-5.5%
NP2-Low Al	SiO_2		30.75	30.58	0.17	0.6%
NP2-Low Al	SO_3		0.25	0.26	-0.01	-3.8%
NP2-Low Al	ZrO_2		0.27	0.26	0.01	3.8%
NP2-Low Al	Sum		98.80	99.63	-0.83	-0.8%
NP2-Low B	Al_2O_3		29.24	29.60	-0.36	-1.2%
NP2-Low B	B_2O_3		13.78	14.00	-0.22	-1.6%
NP2-Low B	Bi_2O_3		0.62	0.68	-0.06	-8.8%
NP2-Low B	CaO		0.63	0.68	-0.05	-7.4%
NP2-Low B	Cr_2O_3		1.04	1.14	-0.10	-8.8%
NP2-Low B	Fe_2O_3		2.64	2.60	0.04	1.5%
NP2-Low B	Li_2O		5.10	5.19	-0.09	-1.7%
NP2-Low B	MnO		0.97	1.04	-0.07	-6.7%
NP2-Low B	Na_2O		13.78	12.98	0.80	6.2%
NP2-Low B	P_2O_5		0.70	0.73	-0.03	-4.1%

Table C.1. Composition Analysis Results Including Reference Material (cont'd)

Glass ID[a]	Oxide	BDL (<)[b]	Measured (mass%)	Targeted (mass%)	Difference of Measured Versus Targeted (mass%)	%Relative Difference of Measured versus Targeted
NP2-Low B	SiO_2		31.07	30.48	0.59	1.9%
NP2-Low B	SO_3		0.23	0.26	-0.03	-11.5%
NP2-Low B	ZrO_2		0.26	0.26	0.00	0.0%
NP2-Low B	Sum		100.06	99.64	0.42	0.4%
NP2-Low Li	Al_2O_3		28.39	28.80	-0.41	-1.4%
NP2-Low Li	B_2O_3		17.25	17.38	-0.13	-0.7%
NP2-Low Li	Bi_2O_3		0.61	0.66	-0.05	-7.6%
NP2-Low Li	CaO		0.63	0.66	-0.03	-4.5%
NP2-Low Li	Cr_2O_3		1.02	1.11	-0.09	-8.1%
NP2-Low Li	Fe_2O_3		2.51	2.53	-0.02	-0.8%
NP2-Low Li	Li_2O		3.80	4.00	-0.20	-5.0%
NP2-Low Li	MnO		0.93	1.01	-0.08	-7.9%
NP2-Low Li	Na_2O		13.36	12.63	0.73	5.8%
NP2-Low Li	P_2O_5		0.66	0.71	-0.05	-7.0%
NP2-Low Li	SiO_2		30.06	29.66	0.40	1.3%
NP2-Low Li	SO_3		0.23	0.25	-0.02	-8.0%
NP2-Low Li	ZrO_2		0.24	0.25	-0.01	-4.0%
NP2-Low Li	Sum		99.69	99.65	0.04	0.0%
NP2-Low Na	Al_2O_3		28.96	29.48	-0.52	-1.8%
NP2-Low Na	B_2O_3		17.31	17.79	-0.48	-2.7%
NP2-Low Na	Bi_2O_3		0.62	0.67	-0.05	-7.5%
NP2-Low Na	CaO		0.55	0.67	-0.12	-17.9%
NP2-Low Na	Cr_2O_3		0.98	1.14	-0.16	-14.0%
NP2-Low Na	Fe_2O_3		2.50	2.59	-0.09	-3.5%
NP2-Low Na	Li_2O		4.81	5.17	-0.36	-7.0%
NP2-Low Na	MnO		0.93	1.03	-0.10	-9.7%
NP2-Low Na	Na_2O		10.19	9.50	0.69	7.3%
NP2-Low Na	P_2O_5		0.68	0.72	-0.04	-5.6%
NP2-Low Na	SiO_2		30.54	30.36	0.18	0.6%
NP2-Low Na	SO_3		0.18	0.26	-0.08	-30.8%
NP2-Low Na	ZrO_2		0.25	0.26	-0.01	-3.8%
NP2-Low Na	Sum		98.50	99.64	-1.14	-1.1%
NP2-Low Si	Al_2O_3		29.57	29.85	-0.28	-0.9%
NP2-Low Si	B_2O_3		18.02	18.02	0.00	0.0%
NP2-Low Si	Bi_2O_3		0.63	0.68	-0.05	-7.4%
NP2-Low Si	CaO		0.55	0.68	-0.13	-19.1%
NP2-Low Si	Cr_2O_3		1.14	1.15	-0.01	-0.9%
NP2-Low Si	Fe_2O_3		2.67	2.62	0.05	1.9%

Table C.1. Composition Analysis Results Including Reference Material (cont'd)

Glass ID[a]	Oxide	BDL (<)[b]	Measured (mass%)	Targeted (mass%)	Difference of Measured Versus Targeted (mass%)	%Relative Difference of Measured versus Targeted
NP2-Low Si	Li_2O		5.14	5.24	-0.10	-1.9%
NP2-Low Si	MnO		1.06	1.05	0.01	1.0%
NP2-Low Si	Na_2O		13.27	13.09	0.18	1.4%
NP2-Low Si	P_2O_5		0.69	0.73	-0.04	-5.5%
NP2-Low Si	SiO_2		26.42	26.00	0.42	1.6%
NP2-Low Si	SO_3		0.22	0.26	-0.04	-15.4%
NP2-Low Si	ZrO_2		0.26	0.26	0.00	0.0%
NP2-Low Si	Sum		99.64	99.63	0.01	0.0%
NP2-Very High Al	Al_2O_3		34.15	34.50	-0.35	-1.0%
NP2-Very High Al	B_2O_3		15.74	15.76	-0.02	-0.1%
NP2-Very High Al	Bi_2O_3		0.55	0.60	-0.05	-8.3%
NP2-Very High Al	CaO		0.56	0.60	-0.04	-6.7%
NP2-Very High Al	Cr_2O_3		0.91	1.01	-0.10	-9.9%
NP2-Very High Al	Fe_2O_3		2.27	2.29	-0.02	-0.9%
NP2-Very High Al	Li_2O		4.35	4.58	-0.23	-5.0%
NP2-Very High Al	MnO		0.84	0.92	-0.08	-8.7%
NP2-Very High Al	Na_2O		12.23	11.45	0.78	6.8%
NP2-Very High Al	P_2O_5		0.61	0.64	-0.03	-4.7%
NP2-Very High Al	SiO_2		27.28	26.89	0.39	1.5%
NP2-Very High Al	SO_3		0.21	0.23	-0.02	-8.7%
NP2-Very High Al	ZrO_2		0.23	0.23	0.00	0.0%
NP2-Very High Al	Sum		99.93	99.70	0.23	0.2%
NP2-Very High Si	Al_2O_3		25.18	25.41	-0.23	-0.9%
NP2-Very High Si	B_2O_3		15.49	15.34	0.15	1.0%
NP2-Very High Si	Bi_2O_3		0.53	0.58	-0.05	-8.6%
NP2-Very High Si	CaO		0.55	0.58	-0.03	-5.2%
NP2-Very High Si	Cr_2O_3		0.92	0.98	-0.06	-6.1%
NP2-Very High Si	Fe_2O_3		2.20	2.23	-0.03	-1.3%
NP2-Very High Si	Li_2O		4.27	4.46	-0.19	-4.3%
NP2-Very High Si	MnO		0.84	0.89	-0.05	-5.6%
NP2-Very High Si	Na_2O		11.61	11.15	0.46	4.1%
NP2-Very High Si	P_2O_5		0.58	0.62	-0.04	-6.5%
NP2-Very High Si	SiO_2		37.49	37.00	0.49	1.3%
NP2-Very High Si	SO_3		0.20	0.22	-0.02	-9.1%
NP2-Very High Si	ZrO_2		0.21	0.22	-0.01	-4.5%
NP2-Very High Si	Sum		100.07	99.68	0.39	0.4%
NP2-Very Low Si	Al_2O_3		31.08	31.46	-0.38	-1.2%
NP2-Very Low Si	B_2O_3		18.80	18.99	-0.19	-1.0%

Table C.1. Composition Analysis Results Including Reference Material (cont'd)

Glass ID[a]	Oxide	BDL (<)[b]	Measured (mass%)	Targeted (mass%)	Difference of Measured Versus Targeted (mass%)	%Relative Difference of Measured versus Targeted
NP2-Very Low Si	Bi_2O_3		0.65	0.72	-0.07	-9.7%
NP2-Very Low Si	CaO		0.58	0.72	-0.14	-19.4%
NP2-Very Low Si	Cr_2O_3		1.13	1.21	-0.08	-6.6%
NP2-Very Low Si	Fe_2O_3		2.83	2.76	0.07	2.5%
NP2-Very Low Si	Li_2O		5.48	5.52	-0.04	-0.7%
NP2-Very Low Si	MnO		1.04	1.10	-0.06	-5.5%
NP2-Very Low Si	Na_2O		14.52	13.80	0.72	5.2%
NP2-Very Low Si	P_2O_5		0.72	0.77	-0.05	-6.5%
NP2-Very Low Si	SiO_2		22.41	22.00	0.41	1.9%
NP2-Very Low Si	SO_3		0.27	0.28	-0.01	-3.6%
NP2-Very Low Si	ZrO_2		0.26	0.28	-0.02	-7.1%
NP2-Very Low Si	Sum		99.77	99.61	0.16	0.2%
NP-MC-AlB-1	Al_2O_3		25.08	25.50	-0.42	-1.6%
NP-MC-AlB-1	B_2O_3		21.77	22.00	-0.23	-1.0%
NP-MC-AlB-1	Bi_2O_3		0.58	0.63	-0.05	-7.9%
NP-MC-AlB-1	CaO		0.51	0.63	-0.12	-19.0%
NP-MC-AlB-1	Cr_2O_3		0.95	1.06	-0.11	-10.4%
NP-MC-AlB-1	Fe_2O_3		2.47	2.42	0.05	2.1%
NP-MC-AlB-1	Li_2O		4.64	4.83	-0.19	-3.9%
NP-MC-AlB-1	MnO		0.87	0.97	-0.10	-10.3%
NP-MC-AlB-1	Na_2O		12.51	12.09	0.42	3.5%
NP-MC-AlB-1	P_2O_5		0.65	0.68	-0.03	-4.4%
NP-MC-AlB-1	SiO_2		28.88	28.38	0.50	1.8%
NP-MC-AlB-1	SO_3		0.24	0.24	0.00	0.0%
NP-MC-AlB-1	ZrO_2		0.24	0.24	0.00	0.0%
NP-MC-AlB-1	Sum		99.39	99.67	-0.28	-0.3%
NP-MC-AlBNa-1	Al_2O_3		26.31	26.80	-0.49	-1.8%
NP-MC-AlBNa-1	B_2O_3		14.95	15.39	-0.44	-2.9%
NP-MC-AlBNa-1	Bi_2O_3		0.67	0.73	-0.06	-8.2%
NP-MC-AlBNa-1	CaO		0.67	0.73	-0.06	-8.2%
NP-MC-AlBNa-1	Cr_2O_3		1.22	1.24	-0.02	-1.6%
NP-MC-AlBNa-1	Fe_2O_3		2.89	2.81	0.08	2.8%
NP-MC-AlBNa-1	Li_2O		5.58	5.62	-0.04	-0.7%
NP-MC-AlBNa-1	MnO		1.14	1.12	0.02	1.8%
NP-MC-AlBNa-1	Na_2O		11.48	10.80	0.68	6.3%
NP-MC-AlBNa-1	P_2O_5		0.76	0.79	-0.03	-3.8%
NP-MC-AlBNa-1	SiO_2		33.21	33.00	0.21	0.6%
NP-MC-AlBNa-1	SO_3		0.27	0.28	-0.01	-3.6%

Table C.1. Composition Analysis Results Including Reference Material (cont'd)

Glass ID[a]	Oxide	BDL (<)[b]	Measured (mass%)	Targeted (mass%)	Difference of Measured Versus Targeted (mass%)	%Relative Difference of Measured versus Targeted
NP-MC-AlBNa-1	ZrO_2		0.29	0.28	0.01	3.6%
NP-MC-AlBNa-1	Sum		99.44	99.59	-0.15	-0.2%
NP-MC-AlBNa-2	Al_2O_3		29.48	29.83	-0.35	-1.2%
NP-MC-AlBNa-2	B_2O_3		19.45	19.32	0.13	0.7%
NP-MC-AlBNa-2	Bi_2O_3		0.53	0.58	-0.05	-8.6%
NP-MC-AlBNa-2	CaO		0.55	0.58	-0.03	-5.2%
NP-MC-AlBNa-2	Cr_2O_3		0.91	0.97	-0.06	-6.2%
NP-MC-AlBNa-2	Fe_2O_3		2.11	2.21	-0.10	-4.5%
NP-MC-AlBNa-2	Li_2O		4.19	4.43	-0.24	-5.4%
NP-MC-AlBNa-2	MnO		0.83	0.89	-0.06	-6.7%
NP-MC-AlBNa-2	Na_2O		14.83	13.83	1.00	7.2%
NP-MC-AlBNa-2	P_2O_5		0.59	0.62	-0.03	-4.8%
NP-MC-AlBNa-2	SiO_2		26.26	26.00	0.26	1.0%
NP-MC-AlBNa-2	SO_3		0.21	0.22	-0.01	-4.5%
NP-MC-AlBNa-2	ZrO_2		0.21	0.22	-0.01	-4.5%
NP-MC-AlBNa-2	Sum		100.15	99.70	0.45	0.5%
NP-MC-AlBSi-1	Al_2O_3		31.46	31.50	-0.04	-0.1%
NP-MC-AlBSi-1	B_2O_3		22.00	22.00	0.00	0.0%
NP-MC-AlBSi-1	Bi_2O_3		0.49	0.53	-0.04	-7.5%
NP-MC-AlBSi-1	CaO		0.43	0.53	-0.10	-18.9%
NP-MC-AlBSi-1	Cr_2O_3		0.82	0.90	-0.08	-8.9%
NP-MC-AlBSi-1	Fe_2O_3		2.09	2.05	0.04	2.0%
NP-MC-AlBSi-1	Li_2O		4.06	4.11	-0.05	-1.2%
NP-MC-AlBSi-1	MnO		0.75	0.82	-0.07	-8.5%
NP-MC-AlBSi-1	Na_2O		10.88	10.27	0.61	5.9%
NP-MC-AlBSi-1	P_2O_5		0.54	0.58	-0.04	-6.9%
NP-MC-AlBSi-1	SiO_2		26.85	26.00	0.85	3.3%
NP-MC-AlBSi-1	SO_3		0.17	0.21	-0.04	-19.0%
NP-MC-AlBSi-1	ZrO_2		0.20	0.21	-0.01	-4.8%
NP-MC-AlBSi-1	Sum		100.74	99.71	1.03	1.0%
NP-MC-AlLi-1	Al_2O_3		24.71	25.50	-0.79	-3.1%
NP-MC-AlLi-1	B_2O_3		17.71	18.23	-0.52	-2.9%
NP-MC-AlLi-1	Bi_2O_3		0.64	0.69	-0.05	-7.2%
NP-MC-AlLi-1	CaO		0.56	0.69	-0.13	-18.8%
NP-MC-AlLi-1	Cr_2O_3		1.14	1.17	-0.03	-2.6%
NP-MC-AlLi-1	Fe_2O_3		2.67	2.65	0.02	0.8%
NP-MC-AlLi-1	Li_2O		3.83	4.00	-0.17	-4.3%
NP-MC-AlLi-1	MnO		1.05	1.06	-0.01	-0.9%

Table C.1. Composition Analysis Results Including Reference Material (cont'd)

Glass ID[a]	Oxide	BDL (<)[b]	Measured (mass%)	Targeted (mass%)	Difference of Measured Versus Targeted (mass%)	%Relative Difference of Measured versus Targeted
NP-MC-AlLi-1	Na_2O		13.39	13.25	0.14	1.1%
NP-MC-AlLi-1	P_2O_5		0.71	0.74	-0.03	-4.1%
NP-MC-AlLi-1	SiO_2		30.86	31.12	-0.26	-0.8%
NP-MC-AlLi-1	SO_3		0.25	0.27	-0.02	-7.4%
NP-MC-AlLi-1	ZrO_2		0.28	0.27	0.01	3.7%
NP-MC-AlLi-1	Sum		97.80	99.64	-1.84	-1.8%
NP-MC-AlLi-2	Al_2O_3		30.99	31.50	-0.51	-1.6%
NP-MC-AlLi-2	B_2O_3		16.40	16.68	-0.28	-1.7%
NP-MC-AlLi-2	Bi_2O_3		0.58	0.63	-0.05	-7.9%
NP-MC-AlLi-2	CaO		0.59	0.63	-0.04	-6.3%
NP-MC-AlLi-2	Cr_2O_3		1.00	1.07	-0.07	-6.5%
NP-MC-AlLi-2	Fe_2O_3		2.40	2.42	-0.02	-0.8%
NP-MC-AlLi-2	Li_2O		3.82	4.00	-0.18	-4.5%
NP-MC-AlLi-2	MnO		0.93	0.97	-0.04	-4.1%
NP-MC-AlLi-2	Na_2O		12.85	12.12	0.73	6.0%
NP-MC-AlLi-2	P_2O_5		0.65	0.68	-0.03	-4.4%
NP-MC-AlLi-2	SiO_2		28.67	28.47	0.20	0.7%
NP-MC-AlLi-2	SO_3		0.21	0.24	-0.03	-12.5%
NP-MC-AlLi-2	ZrO_2		0.24	0.24	0.00	0.0%
NP-MC-AlLi-2	Sum		99.33	99.65	-0.32	-0.3%
NP-MC-AlLiNa-1	Al_2O_3		30.94	31.14	-0.20	-0.6%
NP-MC-AlLiNa-1	B_2O_3		15.15	15.24	-0.09	-0.6%
NP-MC-AlLiNa-1	Bi_2O_3		0.52	0.58	-0.06	-10.3%
NP-MC-AlLiNa-1	CaO		0.53	0.58	-0.05	-8.6%
NP-MC-AlLiNa-1	Cr_2O_3		0.88	0.97	-0.09	-9.3%
NP-MC-AlLiNa-1	Fe_2O_3		2.18	2.21	-0.03	-1.4%
NP-MC-AlLiNa-1	Li_2O		5.70	5.88	-0.18	-3.1%
NP-MC-AlLiNa-1	MnO		0.82	0.89	-0.07	-7.9%
NP-MC-AlLiNa-1	Na_2O		15.70	15.14	0.56	3.7%
NP-MC-AlLiNa-1	P_2O_5		0.58	0.62	-0.04	-6.5%
NP-MC-AlLiNa-1	SiO_2		26.47	26.00	0.47	1.8%
NP-MC-AlLiNa-1	SO_3		0.24	0.22	0.02	9.1%
NP-MC-AlLiNa-1	ZrO_2		0.21	0.22	-0.01	-4.5%
NP-MC-AlLiNa-1	Sum		99.92	99.69	0.23	0.2%
NP-MC-AlLiSi-1	Al_2O_3		25.08	25.50	-0.42	-1.6%
NP-MC-AlLiSi-1	B_2O_3		20.64	20.60	0.04	0.2%
NP-MC-AlLiSi-1	Bi_2O_3		0.72	0.78	-0.06	-7.7%
NP-MC-AlLiSi-1	CaO		0.63	0.78	-0.15	-19.2%

Table C.1. Composition Analysis Results Including Reference Material (cont'd)

Glass ID[a]	Oxide	BDL (<)[b]	Measured (mass%)	Targeted (mass%)	Difference of Measured Versus Targeted (mass%)	%Relative Difference of Measured versus Targeted
NP-MC-AlLiSi-1	Cr_2O_3		1.30	1.32	-0.02	-1.5%
NP-MC-AlLiSi-1	Fe_2O_3		3.02	2.99	0.03	1.0%
NP-MC-AlLiSi-1	Li_2O		3.85	4.00	-0.15	-3.8%
NP-MC-AlLiSi-1	MnO		1.21	1.20	0.01	0.8%
NP-MC-AlLiSi-1	Na_2O		15.91	14.97	0.94	6.3%
NP-MC-AlLiSi-1	P_2O_5		0.79	0.84	-0.05	-6.0%
NP-MC-AlLiSi-1	SiO_2		26.21	26.00	0.21	0.8%
NP-MC-AlLiSi-1	SO_3		0.30	0.30	0.00	0.0%
NP-MC-AlLiSi-1	ZrO_2		0.29	0.30	-0.01	-3.3%
NP-MC-AlLiSi-1	Sum		99.95	99.58	0.37	0.4%
NP-MC-AlNa-1	Al_2O_3		24.94	25.50	-0.56	-2.2%
NP-MC-AlNa-1	B_2O_3		16.58	17.20	-0.62	-3.6%
NP-MC-AlNa-1	Bi_2O_3		0.60	0.65	-0.05	-7.7%
NP-MC-AlNa-1	CaO		0.53	0.65	-0.12	-18.5%
NP-MC-AlNa-1	Cr_2O_3		0.99	1.10	-0.11	-10.0%
NP-MC-AlNa-1	Fe_2O_3		2.49	2.50	-0.01	-0.4%
NP-MC-AlNa-1	Li_2O		4.88	5.00	-0.12	-2.4%
NP-MC-AlNa-1	MnO		0.92	1.00	-0.08	-8.0%
NP-MC-AlNa-1	Na_2O		16.01	15.50	0.51	3.3%
NP-MC-AlNa-1	P_2O_5		0.66	0.70	-0.04	-5.7%
NP-MC-AlNa-1	SiO_2		29.36	29.35	0.01	0.0%
NP-MC-AlNa-1	SO_3		0.25	0.25	0.00	0.0%
NP-MC-AlNa-1	ZrO_2		0.25	0.25	0.00	0.0%
NP-MC-AlNa-1	Sum		98.46	99.65	-1.19	-1.2%
NP-MC-AlSi-1	Al_2O_3		25.04	25.50	-0.46	-1.8%
NP-MC-AlSi-1	B_2O_3		19.62	19.79	-0.17	-0.9%
NP-MC-AlSi-1	Bi_2O_3		0.69	0.75	-0.06	-8.0%
NP-MC-AlSi-1	CaO		0.68	0.75	-0.07	-9.3%
NP-MC-AlSi-1	Cr_2O_3		1.16	1.27	-0.11	-8.7%
NP-MC-AlSi-1	Fe_2O_3		2.93	2.88	0.05	1.7%
NP-MC-AlSi-1	Li_2O		5.58	5.75	-0.17	-3.0%
NP-MC-AlSi-1	MnO		1.07	1.15	-0.08	-7.0%
NP-MC-AlSi-1	Na_2O		15.43	14.38	1.05	7.3%
NP-MC-AlSi-1	P_2O_5		0.77	0.81	-0.04	-4.9%
NP-MC-AlSi-1	SiO_2		26.53	26.00	0.53	2.0%
NP-MC-AlSi-1	SO_3		0.31	0.29	0.02	6.9%
NP-MC-AlSi-1	ZrO_2		0.31	0.29	0.02	6.9%
NP-MC-AlSi-1	Sum		100.12	99.61	0.51	0.5%

Table C.1. Composition Analysis Results Including Reference Material (cont'd)

Glass ID[a]	Oxide	BDL (<)[b]	Measured (mass%)	Targeted (mass%)	Difference of Measured Versus Targeted (mass%)	%Relative Difference of Measured versus Targeted
NP-MC-AlSi-2	Al_2O_3		31.08	31.50	-0.42	-1.3%
NP-MC-AlSi-2	B_2O_3		14.29	14.49	-0.20	-1.4%
NP-MC-AlSi-2	Bi_2O_3		0.50	0.55	-0.05	-9.1%
NP-MC-AlSi-2	CaO		0.54	0.55	-0.01	-1.8%
NP-MC-AlSi-2	Cr_2O_3		0.84	0.93	-0.09	-9.7%
NP-MC-AlSi-2	Fe_2O_3		2.08	2.11	-0.03	-1.4%
NP-MC-AlSi-2	Li_2O		4.00	4.21	-0.21	-5.0%
NP-MC-AlSi-2	MnO		0.76	0.84	-0.08	-9.5%
NP-MC-AlSi-2	Na_2O		11.23	10.53	0.70	6.6%
NP-MC-AlSi-2	P_2O_5		0.55	0.59	-0.04	-6.8%
NP-MC-AlSi-2	SiO_2		33.32	33.00	0.32	1.0%
NP-MC-AlSi-2	SO_3		0.16	0.21	-0.05	-23.8%
NP-MC-AlSi-2	ZrO_2		0.20	0.21	-0.01	-4.8%
NP-MC-AlSi-2	Sum		99.55	99.72	-0.17	-0.2%
NP-MC-BLiSi-1	Al_2O_3		27.40	27.65	-0.25	-0.9%
NP-MC-BLiSi-1	B_2O_3		14.00	14.00	0.00	0.0%
NP-MC-BLiSi-1	Bi_2O_3		0.58	0.63	-0.05	-7.9%
NP-MC-BLiSi-1	CaO		0.51	0.63	-0.12	-19.0%
NP-MC-BLiSi-1	Cr_2O_3		0.97	1.07	-0.10	-9.3%
NP-MC-BLiSi-1	Fe_2O_3		2.41	2.43	-0.02	-0.8%
NP-MC-BLiSi-1	Li_2O		5.76	6.00	-0.24	-4.0%
NP-MC-BLiSi-1	MnO		0.90	0.97	-0.07	-7.2%
NP-MC-BLiSi-1	Na_2O		12.98	12.13	0.85	7.0%
NP-MC-BLiSi-1	P_2O_5		0.64	0.68	-0.04	-5.9%
NP-MC-BLiSi-1	SiO_2		33.59	33.00	0.59	1.8%
NP-MC-BLiSi-1	SO_3		0.21	0.24	-0.03	-12.5%
NP-MC-BLiSi-1	ZrO_2		0.23	0.24	-0.01	-4.2%
NP-MC-BLiSi-1	Sum		100.18	99.67	0.51	0.5%
NP-MC-BLiSi-2	Al_2O_3		26.74	27.06	-0.32	-1.2%
NP-MC-BLiSi-2	B_2O_3		21.90	22.00	-0.10	-0.5%
NP-MC-BLiSi-2	Bi_2O_3		0.57	0.62	-0.05	-8.1%
NP-MC-BLiSi-2	CaO		0.51	0.62	-0.11	-17.7%
NP-MC-BLiSi-2	Cr_2O_3		0.98	1.04	-0.06	-5.8%
NP-MC-BLiSi-2	Fe_2O_3		2.32	2.37	-0.05	-2.1%
NP-MC-BLiSi-2	Li_2O		5.44	6.00	-0.56	-9.3%
NP-MC-BLiSi-2	MnO		0.89	0.95	-0.06	-6.3%
NP-MC-BLiSi-2	Na_2O		12.11	11.87	0.24	2.0%
NP-MC-BLiSi-2	P_2O_5		0.62	0.66	-0.04	-6.1%

Table C.1. Composition Analysis Results Including Reference Material (cont'd)

Glass ID[a]	Oxide	BDL (<)[b]	Measured (mass%)	Targeted (mass%)	Difference of Measured Versus Targeted (mass%)	%Relative Difference of Measured versus Targeted
NP-MC-BLiSi-2	SiO_2		26.42	26.00	0.42	1.6%
NP-MC-BLiSi-2	SO_3		0.24	0.24	0.00	0.0%
NP-MC-BLiSi-2	ZrO_2		0.24	0.24	0.00	0.0%
NP-MC-BLiSi-2	Sum		98.98	99.67	-0.69	-0.7%
NP-MC-BNa-1	Al_2O_3		28.30	28.58	-0.28	-1.0%
NP-MC-BNa-1	B_2O_3		13.87	14.00	-0.13	-0.9%
NP-MC-BNa-1	Bi_2O_3		0.59	0.65	-0.06	-9.2%
NP-MC-BNa-1	CaO		0.60	0.65	-0.05	-7.7%
NP-MC-BNa-1	Cr_2O_3		0.99	1.10	-0.11	-10.0%
NP-MC-BNa-1	Fe_2O_3		2.52	2.51	0.01	0.4%
NP-MC-BNa-1	Li_2O		4.84	5.01	-0.17	-3.4%
NP-MC-BNa-1	MnO		0.92	1.00	-0.08	-8.0%
NP-MC-BNa-1	Na_2O		16.38	15.50	0.88	5.7%
NP-MC-BNa-1	P_2O_5		0.66	0.70	-0.04	-5.7%
NP-MC-BNa-1	SiO_2		30.00	29.43	0.57	1.9%
NP-MC-BNa-1	SO_3		0.26	0.25	0.01	4.0%
NP-MC-BNa-1	ZrO_2		0.25	0.25	0.00	0.0%
NP-MC-BNa-1	Sum		100.18	99.63	0.55	0.6%
NP-MC-BNaSi-1	Al_2O_3		30.66	30.97	-0.31	-1.0%
NP-MC-BNaSi-1	B_2O_3		14.21	14.00	0.21	1.5%
NP-MC-BNaSi-1	Bi_2O_3		0.65	0.71	-0.06	-8.5%
NP-MC-BNaSi-1	CaO		0.66	0.71	-0.05	-7.0%
NP-MC-BNaSi-1	Cr_2O_3		1.17	1.20	-0.03	-2.5%
NP-MC-BNaSi-1	Fe_2O_3		2.72	2.72	0.00	0.0%
NP-MC-BNaSi-1	Li_2O		5.31	5.43	-0.12	-2.2%
NP-MC-BNaSi-1	MnO		1.07	1.09	-0.02	-1.8%
NP-MC-BNaSi-1	Na_2O		16.48	15.50	0.98	6.3%
NP-MC-BNaSi-1	P_2O_5		0.71	0.76	-0.05	-6.6%
NP-MC-BNaSi-1	SiO_2		26.37	26.00	0.37	1.4%
NP-MC-BNaSi-1	SO_3		0.27	0.27	0.00	0.0%
NP-MC-BNaSi-1	ZrO_2		0.26	0.27	-0.01	-3.7%
NP-MC-BNaSi-1	Sum		100.54	99.63	0.91	0.9%
NP-MC-BSi-1	Al_2O_3		25.08	25.50	-0.42	-1.6%
NP-MC-BSi-1	B_2O_3		20.27	20.40	-0.13	-0.6%
NP-MC-BSi-1	Bi_2O_3		0.53	0.58	-0.05	-8.6%
NP-MC-BSi-1	CaO		0.47	0.58	-0.11	-19.0%
NP-MC-BSi-1	Cr_2O_3		0.96	0.98	-0.02	-2.0%
NP-MC-BSi-1	Fe_2O_3		2.27	2.24	0.03	1.3%

Table C.1. Composition Analysis Results Including Reference Material (cont'd)

Glass ID[(a)]	Oxide	BDL (<)[(b)]	Measured (mass%)	Targeted (mass%)	Difference of Measured Versus Targeted (mass%)	%Relative Difference of Measured versus Targeted
NP-MC-BSi-1	Li_2O		4.32	4.47	-0.15	-3.4%
NP-MC-BSi-1	MnO		0.88	0.89	-0.01	-1.1%
NP-MC-BSi-1	Na_2O		12.03	11.18	0.85	7.6%
NP-MC-BSi-1	P_2O_5		0.59	0.63	-0.04	-6.3%
NP-MC-BSi-1	SiO_2		32.30	31.78	0.52	1.6%
NP-MC-BSi-1	SO_3		0.20	0.22	-0.02	-9.1%
NP-MC-BSi-1	ZrO_2		0.21	0.22	-0.01	-4.5%
NP-MC-BSi-1	Sum		100.11	99.67	0.44	0.4%

(a) LRM = Standard Reference Material Glass ID
(b) Less than symbol (<) indicates component concentration is below detectable limits.

Distribution

U.S. Department of Energy

Office of River Protection
AA Kruger

Savannah River National Laboratory
Jake Amoroso
Kevin Fox
Connie Herman
Devon McClane

Washington State University
Ashutosh Goel
Jason Lonergan
Jose Marcial
John McCloy

Pacific Northwest National Laboratory

J Chun	K6-24
SK Cooley	K7-20
JV Crum	K6-24
DR Dixon	K6-28
W Eaton	K6-24
PR Hrma	K6-24
BR Johnson	K6-24
DS Kim	K6-24
CE Lonergan	K6-24
SA Luksic	K6-28
J Matyas	K6-24
B McCarthy	K6-24
ZJ Nelson	K6-24
DK Peeler	K9-09
GF Piepel	K7-20
CP Rodriguez	K6-24
R Russell	K6-24
MJ Schweiger	K6-24
GL Smith	K6-24
J Tongan	K6-24
JD Vienna	K6-24

***All Distribution will be made electronically**

Pacific Northwest
NATIONAL LABORATORY

Proudly Operated by **Battelle** *Since 1965*

U.S. DEPARTMENT OF
ENERGY

902 Battelle Boulevard
P.O. Box 999
Richland, WA 99352
1-888-375-PNNL (7665)

www.pnnl.gov